J. Fluid Mech. (1979), *vol.* 90, *part* 1, *pp.* 33–66
Printed in Great Britain

Radiative interactions in boundary layers

By S. P. VENKATESHAN AND K. KRISHNA PRASAD

Department of Mechanical Engineering,
Indian Institute of Science, Bangalore 560012

(Received 11 April 1977 and in revised form 1 March 1978)

A detailed description of radiative interactions in laminar compressible boundary layers for moderate Mach numbers is presented by way of asymptotic analysis and supporting solutions. The radiation field is described by the differential approximation. While the asymptotic analysis is valid for large N (the ratio of photon mean free path to molecular mean free path) and arbitrary Boltzmann number, Bo (the ratio of convective heat flux to radiation heat flux), the solutions are obtained for $Bo \ll 1$, the case of strong radiative interactions.

The asymptotic analysis shows the existence of an optically thin boundary layer for large N and all Bo. For $Bo \ll 1$, two outer regions are observed – one optically thin (at short distances from the leading edge) and the other optically thick (at large distances from the leading edge). An interesting feature not pointed out in the previous literature is the existence of a wall layer at large distances from the leading edge where convective heat flux can be ignored to the leading order of approximation. The radiation field in all cases can be very well approximated by a one-dimensional description.

The solutions have been constructed using the ideas of matched asymptotic expansions by approximate analytical procedures and numerical methods. It is shown that, to the leading order of approximation, the radiation slip method yields exactly the same result as the more complicated matching procedure. Both the cases of linear and nonlinear radiation have been considered, the former being of interest in developing approximate methods which are subsequently generalized to handle the nonlinear problem. Detailed results are presented for both cases.

1. Introduction

This paper considers the problem of a laminar, compressible, viscous, heat-conducting, radiating, grey gas flow over a semi-infinite plate at zero incidence and uniform temperature. The Mach number of the flow is assumed to be sufficiently large so that viscous dissipation is important, but not large enough to change the thermo-physical properties by orders of magnitude. The main aim is to understand the interaction among the different modes of energy transport in this class of flow. Asymptotic analysis of the problem is carried out and a few solutions in support of the analysis are given.

Intuitively speaking, the long range interaction of radiation tends to flatten temperature profiles. Computations carried out on different systems such as a plane parallel layer with radiation, with radiation and conduction, and optically thick boundary layers (Usiskin & Sparrow 1960; Lick 1963; Sparrow & Cess 1966) bear

abundant testimony to this intuition. This suggests that the thickness of the thermal boundary layer increases considerably in the presence of radiation. Cess (1964) was the first to recognize the singular perturbation nature of the radiative interactions in boundary layers. His arguments were somewhat heuristic and were confined to an incompressible fluid. In spite of these arguments, Viskanta (1966) asserted that the boundary-layer approximations would be valid *only* for optically thick fluids.

A second controversial question concerns the use of a one-dimensional formulation for describing the radiation field. While Viskanta feels that one-dimensionality is inadmissible, Cess (1966) and Pai & Tsao (1966) present criteria (they do not agree with each other) under which one-dimensionality could be justified. These conflicting views cannot be explained by any analysis made so far. The framework of analysis we adopted was originally suggested by Kruskal (1963) and later used by Solan & Cohen (1967*a*, *b*) for the radiating Rayleigh problem. However, there are significant differences between the unsteady one-dimensional (spacewise) Rayleigh problem and the steady two-dimensional nature of the present problem which warrant further study. Moreover, Solan & Cohen interpreted the asymptotic analysis in a rather restrictive manner, totally disregarding the merits of describing the flow field using non-optimal scales (for definition of optimal scales see §2).

We use the differential approximation for describing the radiation field and it is shown that this does not affect the generality of the asymptotic analysis in any way. The asymptotic description is presented in terms of two parameters – N, the ratio of photon mean free path and molecular mean free path, and the Boltzmann number, Bo, the ratio of convective heat flux and the radiative heat flux. For N large, the viscous, heat-conducting boundary layer is always thin. However, the temperature non-uniformity penetrates deep into the inviscid region and the details of energy transfer in this region are determined by Bo.

The non-uniform behaviour of the temperature field demands asymptotic matching of solutions in different regions. If we restrict our attention to leading-order approximations, this matching can be effectively circumvented by the use of slip boundary conditions at the wall. The nonlinear energy equation is solved by an approximate procedure, which in the first instance is justified for the linear problem. The approximate procedure is also validated by obtaining a numerical solution to the problem.

2. Asymptotic analysis

2.1. *Governing equations in dimensionless form*

The governing equations for the problem are the usual Navier–Stokes equations for a compressible fluid with radiation flux terms added to the energy equation [see, for example, Curle (1962) for these equations]. As is customary in this class of problem, we ignore the contributions of radiation pressure in the momentum equations and the radiation energy density in the energy equation.

We use the differential approximation for the exact integro-differential equation of transfer to specify the radiant heat flux. The derivation of the approximation is discussed in detail by Vincenti & Kruger (1965). For the purposes of the present work, it is sufficient to make two comments on the validity of the approximation. The approximation reproduces the behaviour of the exact equation of transfer in the

limits of small and large optical thickness. There appears to be some doubt about the applicability of the approximation to multi-dimensional problems (for a summary of arguments in this connexion, see Sparrow & Cess 1966), though it has been applied to such problems (Cheng 1964). During the course of the asymptotic analysis, we will show that the radiation field is truly one-dimensional at least to the leading order. Hence, the use of the differential approximation will not in any way interfere with the main lines of thought presented in this paper.

We assume that the gas is grey and as such all radiative quantities are integrated quantities. The absorption coefficient has been treated as a constant which is a suitably chosen average. In this part of the work, since the Mach number is not very large, we do not expect variations of temperature across the boundary layer by orders of magnitude. Hence the use of the constant absorption coefficient will neither alter the arguments of the asymptotic analysis nor influence the methodology adopted to construct solutions to the problem. The companion problem of high Mach number taking into account the variation of absorption coefficient with temperature is considered in a separate work (Venkateshan & Krishna Prasad 1978).

The first step in non-dimensionalizing the governing equations is to determine the characteristic measures of the problem. With Mach number asymptotically inactive, the characteristic measures for the thermodynamic and thermophysical properties will be taken as their values in the free stream. The streamwise velocity will also be normalized with respect to the velocity of the oncoming free stream.

However, the above procedure is inapplicable for the length variables (both of which go from 0 to ∞) and the normal velocity (which vanishes at the wall as well as in the free stream). For the length measures, we may use an internal length scale. Two such length scales are available for the present problem – the molecular mean free path and the photon mean free path (defined as the reciprocal of the absorption coefficient). Since our primary interest in this study lies in radiative interactions, we choose to measure lengths in terms of the photon mean free path. This choice by itself will not ensure that the normalized variables will be of order unity in the domain of interest. To achieve this we introduce two non-dimensional scaling parameters in the definitions of these normalized variables. A similar strategy is adopted while normalizing the normal component of velocity with respect to the free-stream velocity. One of the purposes of the asymptotic analysis could be thought of as the determination of these scaling parameters.

Non-dimensional variables (without primes), all of order unity, are introduced through the following definitions:

$$\left.\begin{aligned} x' &= \bar{x}\beta_1\lambda'_{ph\infty}, & y' &= \bar{y}\beta_2\lambda'_{ph\infty}, & & \\ u' &= uu'_\infty, & v' &= v\beta_3 u'_\infty, & & \\ \mu' &= \mu\mu'_\infty, & \bar{\mu}' &= \bar{\mu}\mu'_\infty, \quad k' = kk'_\infty, & \alpha' &= \alpha\alpha'_\infty, \\ p' &= pp'_\infty, & \rho' &= \rho\rho'_\infty, \quad T' = TT'_\infty, & h' &= hh'_\infty, \\ q'_{Rx} &= \bar{q}_{xR}\sigma T'^4_\infty, & q'_{Ry} &= \bar{q}_{Ry}\sigma T'^4_\infty, & & \end{aligned}\right\} \tag{1}$$

where u' and v' are the components of the velocity parallel to x' and y' respectively, ρ' is the density, p' the pressure, μ' the viscosity, $\bar{\mu}' = \mu' + \frac{3}{4}\mu'_B$ with μ'_B the bulk viscosity, T' the temperature, h' the enthalpy, k' the thermal conductivity, q'_{Rx} and q'_{Ry} the radiant fluxes in the x' and y' directions respectively, α' is the absorption coefficient,

σ is the Stefan–Boltzmann constant and the subscript ∞ refers to the free-stream conditions.

Introducing the non-dimensional variables defined above into the basic equations and the boundary conditions we get:

$$\frac{\partial \rho u}{\partial \bar{x}} + \frac{\beta_1\beta_3}{\beta_2}\frac{\partial \rho v}{\partial \bar{y}} = 0, \tag{2a}$$

$$\rho\left[u\frac{\partial u}{\partial \bar{x}} + \frac{\beta_1\beta_3}{\beta_2}v\frac{\partial u}{\partial \bar{y}}\right] = -\frac{A_1}{A_2}\frac{\partial p}{\partial \bar{x}} + \frac{1}{N\beta_1}\frac{\partial}{\partial \bar{x}}\left[\bar{\mu}\left(\frac{\partial u}{\partial \bar{x}} + \frac{\beta_1\beta_3}{\beta_2}\frac{\partial v}{\partial \bar{y}}\right)\right] + \frac{2}{N\beta_1}\frac{\partial}{\partial \bar{x}}\left(\mu\frac{\partial u}{\partial \bar{x}}\right) + \frac{1}{N\beta_2^2}\frac{\partial}{\partial \bar{y}}\left[\mu\left(\frac{\partial u}{\partial \bar{y}} + \frac{\beta_3\beta_2}{\beta_1}\frac{\partial v}{\partial \bar{x}}\right)\right], \tag{2b}$$

$$\rho\left[u\frac{\partial v}{\partial \bar{x}} + \frac{\beta_1\beta_3}{\beta_2}v\frac{\partial v}{\partial \bar{y}}\right] = -\frac{A_1}{A_2}\frac{\beta_1}{\beta_2\beta_3}\frac{\partial p}{\partial \bar{y}} + \frac{1}{N\beta_2\beta_3}\frac{\partial}{\partial \bar{y}}\left[\bar{\mu}\left(\frac{\partial u}{\partial \bar{x}} + \frac{\beta_3\beta_1}{\beta_2}\frac{\partial v}{\partial \bar{y}}\right)\right] + 2\frac{1}{N\beta_2^2}\frac{\partial}{\partial \bar{y}}\left(\mu\frac{\partial v}{\partial \bar{y}}\right) + \frac{1}{N\beta_1}\frac{\partial}{\partial \bar{x}}\left[\mu\left(\frac{\partial v}{\partial \bar{x}} + \frac{\beta_1}{\beta_2\beta_3}\frac{\partial u}{\partial \bar{y}}\right)\right], \tag{2c}$$

$$\rho\left[u\frac{\partial h}{\partial \bar{x}} + \frac{\beta_1\beta_3}{\beta_2}v\frac{\partial h}{\partial \bar{y}}\right] - A_1\left[u\frac{\partial p}{\partial \bar{x}} + v\frac{\partial p}{\partial \bar{y}}\right] = \frac{A_3}{N\beta_1}\frac{\partial}{\partial \bar{x}}\left(k\frac{\partial T}{\partial \bar{x}}\right) + \frac{A_3\beta_1}{N\beta_2^2}\frac{\partial}{\partial \bar{y}}\left(k\frac{\partial T}{\partial \bar{y}}\right) + \left[A_2\mu\frac{2}{N\beta_1}\left(\frac{\partial u}{\partial \bar{x}}\right)^2 + \frac{1}{N\beta_2^2}\left(\frac{\partial u}{\partial \bar{y}}\right)^2 + \frac{2\beta_3}{N\beta_2}\frac{\partial u}{\partial \bar{y}}\frac{\partial v}{\partial \bar{x}} + \frac{\beta_3^2}{N\beta_1}\left(\frac{\partial v}{\partial \bar{x}}\right)^2 + \frac{2\beta_1\beta_3^2}{N\beta_2^2}\left(\frac{\partial v}{\partial \bar{y}}\right)^2\right] - \frac{\beta_1}{Bo}\left[\frac{1}{\beta_1}\frac{\partial \bar{q}_{Rx}}{\partial \bar{x}} + \frac{1}{\beta_2}\frac{\partial \bar{q}_{Ry}}{\partial \bar{y}}\right], \tag{2d}$$

$$\frac{\partial}{\partial \bar{x}}\left(\frac{\partial \bar{q}_{Rx}}{\partial \bar{x}} + \frac{\beta_1}{\beta_2}\frac{\partial \bar{q}_{Ry}}{\partial \bar{y}}\right) = 3(\rho\alpha)^2\beta_1^2\bar{q}_{Rx} + 4(\rho\alpha)\beta_1\frac{\partial T^4}{\partial \bar{x}}, \tag{2e}$$

$$\frac{\partial}{\partial \bar{y}}\left(\frac{\partial \bar{q}_{Rx}}{\partial \bar{x}} + \frac{\beta_1}{\beta_2}\frac{\partial \bar{q}_{Ry}}{\partial \bar{y}}\right) = 3(\rho\alpha)_2\beta_1\beta_2\bar{q}_{Ry} + 4(\rho\alpha)\beta_1\frac{\partial T^4}{\partial \bar{y}}, \tag{2f}$$

with
$$u(\bar{x},0) = v(\bar{x},0) = 0, \quad u(\bar{x},\infty) = u(0,\bar{y}) = 1,$$
$$v(0,\bar{y}) = v(\bar{x},\infty) = 0, \quad T(\bar{x},0) = 1/\Delta, \quad T(\bar{x},\infty) = T(0,\bar{y}) = 1, \tag{2g}$$
$$\bar{q}_{Rx}(0,\bar{y}) = \bar{q}_{Rx}(\bar{x},\infty) = \bar{q}_{Rx}(\bar{x},0) = 0,$$
$$\bar{q}_{Ry}(0,\bar{y}) = \bar{q}_{Ry}(\bar{x},\infty) = 0,$$
$$\bar{q}_{Ry}(\bar{x},0) = \bar{q}_{RW}, \tag{2h}$$

where $\Delta = T'_\infty/T'_W$, and the subscript W refers to the plate surface.

The following non-dimensional parameters appear in the above system of equations:

$$N = \frac{u'_\infty \lambda'_{ph\infty}}{\nu'_\infty}, \quad Bo = \frac{\rho'_\infty u'_\infty h'_\infty}{\sigma T'^4_\infty},$$
$$A_1 = \frac{p'_\infty}{\rho'_\infty h'_\infty}, \quad A_2 = \frac{u'^2_\infty}{h'_\infty}, \quad A_3 = \frac{k'_\infty T'_\infty}{\mu'_\infty h'_\infty}. \tag{3}$$

For an ideal gas and Mach number of order unity, A_1, A_2 and A_3 are all of order unity and will not enter into any further discussions on the asymptotics. N is seen to be a Reynolds number based on $\lambda_{ph\infty}$ as the characteristic length.

For the present problem, N can also be thought of as a ratio of the two internal

length scales of the problem. (This follows from the kinetic theory.) *Bo*, the Boltzmann number, represents the ratio of a reference convective enthalpy flux and a reference radiative enthalpy flux, and thus determines the relative importance of the processes of convection and radiation in a given situation. It is easy to show that the different dimensionless parameters employed in the literature can all be expressed in terms of N, Bo and the conventional convective heat transfer parameters (Venkateshan 1977).

The choice of the asymptotics in terms of N and Bo is guided by the high temperature property calculations presented for air by Sibulkin & Dennar (1972) and Venkateshan & Krishna Prasad (1975), for CO_2, H_2O and NH_3 by Cess (1966), and for CO_2 by Ozisik (1973). From these it is concluded that the asymptotics corresponding to $N \gg 1$ and arbitrary Bo would be of engineering interest. The authors consider all other possible asymptotics for the problem elsewhere (Venkateshan & Krishna Prasad 1973).

2.2. *Asymptotic analysis for* $N \to \infty$

We adopt the formal approach first developed by Kruskal (1963) and later used by Solan & Cohen (1967*a*, *b*) for the asymptotic analysis. The method is particularly convenient for problems where multiple parameters are involved in the asymptotic analysis. The method is called by Kruskal 'the principle of maximal complication' or 'the principle of minimal simplifications'. The procedure is a systematic means by which asymptotic forms of the governing equations can be constructed without losing any essential physical information in the problem. In practice, it reduces to the determination of the scaling parameters β_1, β_2 and β_3.

We first note, from the process of normalization, that the measure of each term in the equations (2*a*) to (2*f*) is given by the coefficient of the derivatives concerned. From this, it follows that the equation of continuity will be preserved if

$$\beta_1\beta_3/\beta_2 = O(1).$$

Using this relation and grouping terms of the same measure, the following ordering relations result for the momentum and energy equations:

$$x \text{ momentum} \div 1 : \frac{1}{N\beta_1} : \frac{\beta_1}{N\beta_2^2}, \tag{4a}$$

$$y \text{ momentum} \div 1 : \frac{\beta_1^2}{\beta_2^2} : \frac{1}{N\beta_1} : \frac{\beta_1}{N\beta_2^2}, \tag{4b}$$

$$\text{Energy} \div 1 : \frac{1}{N\beta_1} : \frac{\beta_1}{N\beta_2^2} : \frac{\beta_2^2}{N\beta_1^3} : \frac{\beta_1}{Bo} f_1(\beta_1) : \frac{\beta_1}{Bo} f_2(\beta_2), \tag{4c}$$

where $f_1(\beta_1)$ and $f_2(\beta_2)$ are functions to be determined later.

Before proceeding further, it might be worth associating physical meanings with each of the above terms. The first term in each of the equations represents the convective terms; $1/N\beta_1$, the diffusion and dissipative effects in the streamwise direction; $\beta_1/N\beta_2^2$, the same effects as above, but in the normal direction; β_1^2/β_2^2 turns out to be the pressure gradient term in the normal direction; $\beta_2^2/N\beta_1^3$ represents the dissipative effects due to the gradient of v in the streamwise direction; the terms involving Bo determine the radiative effects. Before turning to the actual asymptotic analysis, we will investigate the nature of the functions $f_1(\beta_1)$ and $f_2(\beta_2)$.

For $\beta_1 \ll 1$ and $\beta_2 \ll 1$, dividing by β_1, $(2e)$ and $(2f)$ reduce to

$$\frac{1}{\beta_1}\frac{\partial \bar{q}_{Rx}}{\partial \bar{x}} + \frac{1}{\beta_2}\frac{\partial \bar{q}_{Rx}}{\partial \bar{y}} = O(T^4) = O(1). \tag{5}$$

The last part of the equation follows from the normalization procedure. Equation (5) is the emission dominant or the optically thin limit. Thus the radiation terms in the energy equation are scaled as β_1/Bo. However, there are two terms, the ratio of which is given by:

$$\frac{\partial \bar{q}_{Rx}}{\partial \bar{x}} \Big/ \frac{\partial \bar{q}_{Rx}}{\partial \bar{y}} = O\left(\frac{\beta_2}{\beta_1}\right) = O(\bar{q}_{Rx}/\bar{q}_{Ry}), \tag{6}$$

requiring $\beta_1 \gg \beta_2$ for one-dimensionality of the radiation field.

For $\beta_1 \gg 1$ and $\beta_2 \gg 1$, with the same operations as before, we get

$$\bar{q}_{Rx} = -\frac{4}{3\rho\alpha}\frac{1}{\beta_1}\frac{\partial T^4}{\partial \bar{x}}, \quad \bar{q}_{Ry} = \frac{4}{3\rho\alpha}\frac{1}{\beta_2}\frac{\partial T^4}{\partial \bar{y}}, \tag{7}$$

and

$$f_1(\beta_1) = 1/\beta_1^2, \quad f_2(\beta_2) = 1/\beta_2^2. \tag{8}$$

Equation (8) is the diffusion approximation for the radiation. It is easy to see from (8) that the same criterion for one-dimensionality of the radiation field is obtained in this limit as well. The above results may be summarized by

$$f_1(\beta_1) = \min(1, \beta_1^{-2}), \tag{9}$$

$$f_2(\beta_2) = \min(1, \beta_2^{-2}). \tag{10}$$

Other possible limits for the problem ($\beta_1 \ll 1$, $\beta_2 \gg 1$ and $\beta_1 \gg 1$, $\beta_2 \ll 1$) do not yield any new physical information. The same limiting forms as scales (9) and (10) are obtained by using the exact equation of transfer (see Solan & Cohen 1967*a*), thus proving that the use of the differential approximation does not invalidate the generality of the asymptotic analysis presented here.

We now return to the relations $(4a)$ to $(4c)$. A set of 24 order equalities are generated by equating every possible pair of terms. Many of them are repetitive and the following is a list of independent equalities generated by the procedure:

$$\left.\begin{array}{llllll}
A. & N\beta_1 = 1,\dagger & & & & \\
B. & N\beta_2^2 = \beta_1, & & & & \\
C. & \beta_1 = \beta_2, & & & & \\
D. & N\beta_1^3 = \beta_2^2, & & & & \\
E. & \beta_1 = Bo, & \beta_1 < 1; & Bo\beta_1 = 1, & \beta_1 > 1, \\
F. & \beta_1 = Bo, & \beta_2 < 1; & Bo\beta_2^2 = \beta_1, & \beta_2 > 1, \\
G. & N\beta_1^2 = Bo, & \beta_1 < 1; & N = Bo, & \beta_1 > 1, \\
H. & N\beta_1^2 = Bo, & \beta_2 < 1; & N\beta_1^2 = Bo\beta_2^2, & \beta_2 > 1, \\
I. & N\beta_2^2 = Bo, & \beta_1 < 1; & N\beta_1^2 = Bo\beta_2^2, & \beta_1 > 1, \\
J. & N\beta_2^2 = Bo, & \beta_2 < 1; & N = Bo, & \beta_2 > 1, \\
K. & N\beta_1^4 = \beta_2^2 Bo, & \beta_1 < 1; & N\beta_1^2 = Bo\beta_2^2, & \beta_1 > 1, \\
L. & N\beta_1^4 = \beta_2^2 Bo, & \beta_2 < 1; & N\beta_1^4 = \beta_2^4 Bo, & \beta_2 > 1.
\end{array}\right\} \tag{11}$$

† These equalities should be read as: $N\beta_1$ is of order unity; $\beta_1 < 1$ implies β_1 is very much smaller than unity, etc.

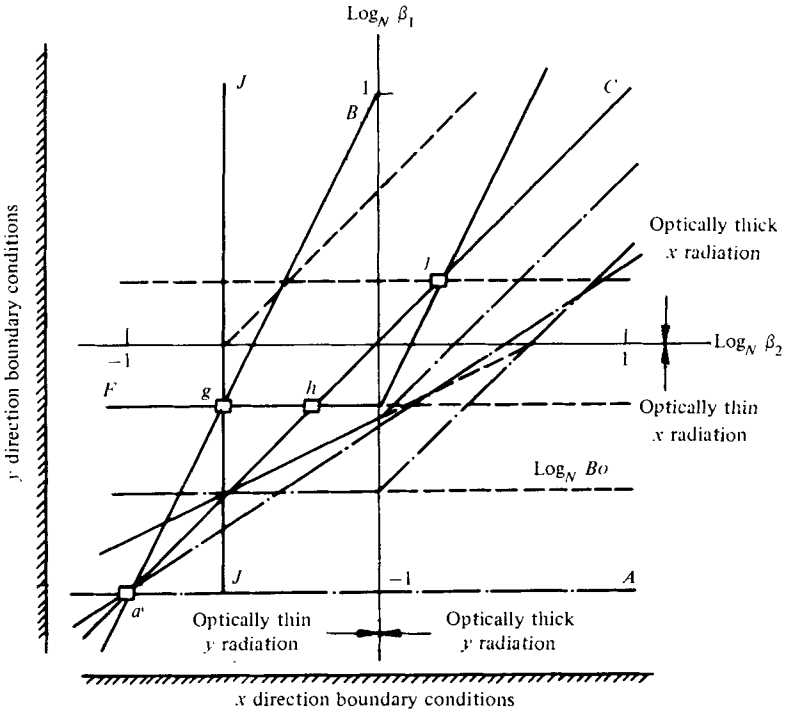

FIGURE 1. Ordering scheme of the complete system of equations. ——, dominant equalities; -·-·-, second-order y radiation effects; – – –, x radiation effects.

In the above, certain repetitive equalities arising in connexion with radiative terms have been included for the sake of clarity in further discussion.

Before proceeding further, it is necessary to specify the range of the Boltzmann number to be considered. In agreement with Solan & Cohen we choose $Bo \gg N^{-1}$ since the problem cannot be treated by the continuum description for $Bo < N^{-1}$. With the case $Bo \gg N$ treated elsewhere (Venkateshan & Krishna Prasad 1973) we chose the range $N^{-1} \ll Bo \ll N$ for the present treatment.

Having chosen the range of Bo, each of the relations (11) can be most conveniently plotted as a line on a $\log_N \beta_1 - \log_N \beta_2$ graph. Figure 1 shows such a plot for $Bo \ll 1$. (Similar plots can be prepared for $Bo = O(1)$ and $Bo \gg 1$.) Each line in the plot can be associated with a physical meaning by tracing its genesis to the original equations. We consider two examples to illustrate this. The order equality $N\beta_1 = 1$ is represented by line A in the figure. In the limit $N \to \infty$, the diffusion effects in the y direction dominate those in the x direction in the region above line A. The order equality $\beta_1 = Bo$ in the half-plane $\beta_2 < 1$ is represented by the line F. On this line convection and radiation effects are of the same order of magnitude. In the region above the line, convection effects are of a lower order of magnitude and can be ignored to the leading order. In the region below this line, the reverse situation prevails. These ideas can be utilized to simplify the governing equations for each of these regions.

It can be easily seen that the lines A, B, C and D correspond to the conventional compressible laminar boundary-layer problem. The boundary-layer simplification is valid everywhere along the line B (above line A) except in the vicinity of the point of

	Region a	Region g	Region h	Region j
β_1	N^{-1}	Bo	Bo	Bo^{-1}
β_2	N^{-1}	$(Bo/N)^{\frac{1}{2}}$	Bo	Bo^{-1}
β_3	1	$(BoN)^{-\frac{1}{2}}$	1	1
x'	$\lambda'_{mfp\,\infty}$	$Bo\lambda'_{ph\,\infty}$	$Bo\lambda'_{ph\,\infty}$	$Bo^{-1}\lambda'_{ph\,\infty}$
y'	$\lambda'_{mfp\,\infty}$	$(Bo/N)^{\frac{1}{2}}\lambda'_{ph\,\infty}$	$Bo\lambda'_{ph\,\infty}$	$Bo^{-1}\lambda'_{ph\,\infty}$
v'	u'_∞	$(BoN)^{-\frac{1}{2}}u'_\infty$	u'_∞	u'_∞
τ	N^{-1}	$(BoN)^{\frac{1}{2}}$	Bo	Bo^{-1}
Physical description	Molecular mean free path region; no radiation effects	Optically thin boundary layer; one-dimensional radiation	Inviscid optically thin region; two-dimensional radiation	Inviscid optically thick region; two-dimensional radiation

Notes:

(i) The order symbols have been suppressed for convenience.

(ii) τ, optical thickness, $= \int_0^{y'} \rho'\alpha' dy'$; λ'_{mfp} and λ'_{ph} are the molecular and photon mean free path respectively.

(iii) For $Bo = O(1)$, no changes are observed in regions a and g. h and j coalesce into a single region. This easily follows from figure 1. No simplification is possible in the equation of transfer in this coalesced scaling.

(iv) For $Bo \gg 1$, only regions a and g appear. Again this can be deduced from figure 1 by shifting line F to a point above $\log_N \beta_2$ axis.

(v) See text for a fuller discussion on the two-dimensionality of the radiation field in regions h and j.

TABLE 1. Summary of optimal scales: $N \gg 1$ and $Bo \ll 1$.

intersection of all these lines. One other point worthy of note in this connexion is the role played by the line C which represents the order equality $\beta_1 = \beta_2$. Along this line, the x direction viscous, conduction and radiation terms are of the same order as the corresponding y direction terms. To the left of this line y direction terms dominate to the leading order and the x terms to the right of this line. This means that all disturbances due to the presence of the body will die down to the far right of this line. For the radiationless problem, a scale on line B represents the boundary layer and a scale on line C, the inviscid outer flow.

All other lines in the graph arise from the presence of radiation. These lines intersect the lines A, B, C and D at different points. The scalings corresponding to those points of intersection that retain the maximum number of terms while accomplishing considerable simplifications in the original set of equations are designated as 'optimal' scalings by Solan & Cohen. (These should not be confused with the 'optimal coordinates' introduced by Kaplun 1954.) These optimal scales are determined by the principle of minimal simplification enunciated by Kruskal (1963).

The optimal scales for the problem are presented in table 1. The simplifications that result from these scales can easily be derived from equations (2a) to (2f) and are not reproduced here for the sake of brevity.

3. Discussion of asymptotic behaviour for $N \gg 1$

3.1. *The optimal regions*

We now discuss the physical and mathematical consequences of the asymptotic analysis presented above. It is seen that in the limit $N \gg 1$ the mean free-path region is free of radiative interaction to the leading order. This region is defined by the complete Navier–Stokes equations and is mathematically difficult to handle. In conformity with the practice followed in this class of problem we assume that it is not necessary to solve the flow in this region to provide boundary conditions for the other regions.† The mean free-path region pertains to the flow prevailing in the vicinity of the leading edge and the above assumption amounts to saying that the flow in the regions downstream is relatively insensitive to the details of flow near the leading edge. This region is similar to the mean free-path, mean free-time region of the radiating Rayleigh problem of Solan & Cohen.

The nature of the radiative interactions downstream of the mean free-path region is best understood on the physical plane. For this purpose we note that the

$$\log_N \beta_1 - \log_N \beta_2$$

plane is a map of the physical plane, which is the region $x' > 0, y' > 0$ above the plate. Moving upward along the β_1 direction from point a in figure 1 is equivalent to moving along the streamwise direction, and similarly moving along the β_2 direction corresponds to movement normal to the plate surface. Using this idea, it is possible to construct a schematic representation (figure 2) of the various regimes of radiative interaction which appear in the present problem. This figure has been constructed for $N \gg 1$ and $Bo \ll 1$. It is interesting to see that a consequence of increasing Bo is simply to shift region g to the right of its present location. In other words, a larger region of the flow is free of radiative effects to the leading order. The length scale $\lambda'_{ph\infty}$ is also marked on the figure. For ready reference, figure 1 is drawn as an inset, with only the dominant lines on it.

The heavily shaded regions correspond to the points of intersection g, h and j. Region g is the conventional boundary layer (also the conventional thermal boundary layer since $Pr \simeq 1$). Regions h and j are in the inviscid, non-conducting flow field with radiation and convection equally important. These are the optimal regions in the Kruskal formalism as employed by Solan & Cohen. The order of magnitude of τ, the optical thickness, increases monotonically from region a to j and spans the entire range from a non-participating to an opaque medium.

We next consider the question of the dimensionality of the radiation field. Region a is free from radiation interaction and hence the isothermal condition of the flow far from the plate is maintained. Thus there is no component of radiation imposed by this region as the gas flows across it. Radiative interaction achieves importance over the scale g, the optically thin boundary layer. The radiation field in this region is one-dimensional in the y direction. The outer regions h and j are coupled two-fold with g, firstly by the transverse velocity generated in the boundary layer, and secondly by the radiation from the wall and the boundary layer. It is well known that the transverse velocity generated by the boundary layer is small and can be ignored to the

† The justification for such a procedure rests on the work of Howarth (1951) on the compressible Rayleigh problem.

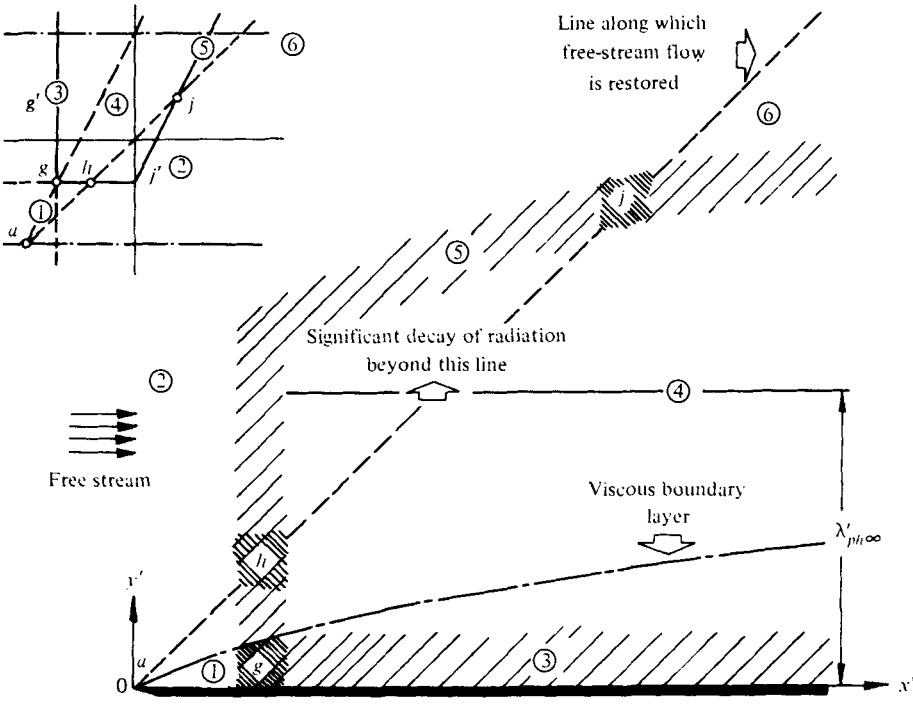

FIGURE 2. Schematic representation of variations regions of radiative interactions. ①, convection + conduction; ②, radiation weak; ③, conduction + radiation; ④, radiation dominant; ⑤, convection + radiation; ⑥, convection dominant.

leading order of the approximation. A similar situation prevails as regards the optically thin radiation from the boundary layer. Thus, it is only the wall radiation which excites the field outside g.

One feature that distinguishes the two outer regions from the boundary layer is that they lie on the line $\beta_1 = \beta_2$ and hence x and y radiation effects must be equally important. It thus appears that the one-dimensional approximation for the radiation field breaks down in the outer layers. However, from the comments in the last paragraph, the only source of radiation important to the leading order is one-dimensional radiation from the plate. There is no source of radiation in the x direction and scattering is not included in the present study. For these reasons, the radiation field in the outer layers is also forced to be one-dimensional. These arguments clearly set at rest the doubts expressed by Viskanta (1966) about the validity of the one-dimensional approximation for the radiation field.

From the above discussions the points of similarity between the present work and that of Solan & Cohen become obvious. However, differences arise because the radiating Rayleigh problem is a naturally one-dimensional problem while the present one is not. The one-dimensional feature of the radiation field in the present case is essentially an approximation. The second point of difference arises in the outer inviscid flow. In the Rayleigh problem, the outer flow behaves like a traditional piston problem. In linearized flows it is conventional to draw an analogy between the time variable in a piston problem and the x variable in a slightly perturbed two-dimensional flow

field. Thus it is a commonly understood fact that the x variable in a linearized two-dimensional inviscid flow acts as a 'time-like' variable. In the presence of radiation, this analogy breaks down even for linearized inviscid flows (Vincenti & Kruger 1965).

The cases $Bo = O(1)$ and $Bo \gg 1$ can be treated together now. The viscous boundary layer in both the cases is again optically thin and one-dimensional. Thus, for $N \to \infty$, Bo finite and Mach number asymptotically inactive, the viscous boundary layer is optically thin and the radiation field is one-dimensional to the leading order. For $Bo = O(1)$ only one optimal region appears in the outer inviscid flow. The two regions one observes for $Bo \ll 1$ coalesce into a single region. The optical thickness is of order unity and the full equation of transfer has to be used to describe the radiation field. For the one-dimensionality of the outer field the arguments similar to those used for $Bo \ll 1$ have to be invoked. For $Bo \gg 1$, no optimal asymptotic scale in the outer field can be defined in the framework of the present analysis.

3.2. *Some non-optimal regions*

Now we turn our attention to interesting details which can be obtained from figure 2. These pertain to several regions which are not optimal in the sense considered so far. Being optically thin regions g and h allow the wall radiation to go unattenuated into a region outside it. Sufficient decay of radiation is imperative before we move out into region 2 where no radiation is present. There is thus a region corresponding to the scales on the horizontal line through g and h (in the inset) where the wall radiation decays to the zero value in 2. As can be seen from the sketch, only radiation and convection balance each other in this region, and the optical thickness is of order unity corresponding to the scaling j'.

While the transition from optically thin conditions of region h to optically thick conditions of region j is taking place in the outer inviscid region, the inner flow undergoes an interesting transition from a viscous heat-conducting radiating boundary layer to a non-optimal conduction layer represented by 3. Here conduction and radiation balance each other and the gas is at rest to the leading order. This region is however optically thin, requiring the optically thick scales j over which wall radiation finds significant attenuation. Corresponding to the conduction layer on 3 the conventional boundary layer shows no interesting feature, being radiation dominant. As opposed to the parabolic growth of the boundary layer, the conduction layer is of constant thickness.

The scalings for the regions discussed above are presented in table 2. Again, the simplified equations are suppressed for brevity. This completes the description of the flow field. In §4, we demonstrate the use of these regions – both optimal and non-optimal – to construct solutions to the problem.

We would like to emphasize the role of these non-optimal scales in constructing solutions by specifically drawing attention to the fact that the location of region g along the plate is dependent on the value of Bo. For large Bo, a significant proportion of the flow field (left of region g in figure 2) is free of radiative interactions to the leading order. For constructing solutions to such situations, it seems unnecessarily complicated to use optimal scales. In fact these non-optimal scales have been employed to construct solutions for the weakly radiating problem elsewhere (Venkateshan 1977).

	Region j'	Region g'	Region g''
β_1	Bo	$1/Bo$	$1/Bo$
β_2	1	$(Bo/N)^{\frac{1}{2}}$	$(BoN)^{-\frac{1}{2}}$
β_3	$1/Bo$	$Bo(Bo/N)^{\frac{1}{2}}$	$(Bo/N)^{\frac{1}{2}}$
x'	$Bo\lambda'_{ph\infty}$	$\lambda'_{ph\infty}/Bo$	$\lambda'_{ph\infty}/Bo$
y'	$\lambda'_{ph\infty}$	$\lambda'_{ph\infty}(Bo/N)^{\frac{1}{2}}$	$\lambda'_{ph\infty}(BoN)^{-\frac{1}{2}}$
v	u'_∞/Bo	$u'_\infty Bo(Bo/N)^{\frac{1}{2}}$	$u'_\infty(Bo/N)^{\frac{1}{2}}$
τ	1	$(Bo/N)^{\frac{1}{2}}$	$(BoN)^{-\frac{1}{2}}$
Physical description	Inviscid, non-heat-conducting optically finite region	Optically thin conduction layer	Radiation dominant optically thin boundary layer

Note: See notes (i) and (ii) under table 1 for symbols.

TABLE 2. Some non-optimal scales: $N \gg 1$ and $Bo \ll 1$.

3.3. *Comparison with earlier work*

The model developed by Cess can now be interpreted in terms of the present scalings. It can be shown that the conduction radiation interaction parameter N_{CR} can be expressed in terms of N and Bo as $(1/4Pr)(Bo/N)$. The range $N^{-1} \ll Bo \ll N$ then corresponds to $N^{-2} \ll N_{CR} \ll 1$. The Cess limit of $N_{CR} \to 0$ is in complete agreement with the present limit $N \to \infty$ and Bo finite. The Cess limit, in common with the present work, physically implies a weakly conducting medium. The main drawback of the Cess limit is that it obscures the central role played by the Boltzmann number. In particular the nature of the outer inviscid region is not clearly delineated. This is an obvious consequence of the choice of the conduction–radiation parameter as central to the analysis. Cess suggests that the viscous boundary layer is optically thin by purely intuitive arguments based on the fact that this layer is physically thin. The result comes out naturally from the asymptotic analysis presented here. Furthermore, the criterion for the one-dimensionality deduced by Cess, viz.

$$u'_\infty L/(16\sigma T'^3_\infty/3\alpha'_\infty \rho'_\infty C'_p) \gg 1,\dagger$$

assumes an optically thick expression for the radiative flux. This expression may be rephrased, using the present variables as $Bo^2(x_L/N.Bo) \gg 1$, where x_L is the Reynolds number based on the length L of the plate. It can easily be shown that the term in the bracket is ξ_L,‡ leading to $Bo^2\xi_L \gg 1$. In the present case $\xi_L = O(1)$ and thus the criterion for one-dimensionality reduces to $Bo \gg 1$, corresponding to the case of a weakly radiating flow (see Venkateshan 1977). This is a highly restrictive condition in the light of the arguments presented earlier. Clearly, the Cess result must be attributed to the choice of the optically thick flux expression as the characteristic flux for an optically thin gas.

The criterion for one-dimensionality given by Pai & Tsao can be shown to require that $\xi_L \ll 1$, for Pr of order unity. As can be seen from the above, this criterion again is very restrictive in that it requires negligible interaction between radiation and convection.

† C'_p is the specific heat at constant pressure.
‡ ξ_L is the Cess variable defined by $\xi = 2\sigma\alpha'_\infty T'^3_\infty x'/\rho'_\infty C'_p u'_\infty$.

4. Solution for $N \gg 1$ and $Bo \ll 1$

4.1. *The governing equations*

The asymptotic analysis presented above indicates that the momentum equations for the problem reduce to the conventional boundary-layer form. Restricting the problem to a perfect gas with constant specific heat, viscosity and thermal conductivity varying linearly with temperature, and Prandtl number constant at unity reduces these equations to the Blasius equation whose solution is known (Schlichting 1960). In the rest of the work, we will concentrate only on the energy equation and the equation of transfer.

To the leading order we can show that the optically thin inviscid region h and also the radiation dominant boundary layer g'' are isothermal. Hence we ignore these regions in the following treatment. In common with the Blasius equation the similarity variable,

$$\eta \left(\equiv \frac{1}{2x^{\frac{1}{2}}} \int_0^y \frac{\rho'}{\rho'_\infty} dy, \quad x \equiv \frac{u'_\infty x'}{\nu'_\infty} \right),$$

is chosen as one of the independent variables. Noting that radiation convection interaction becomes important over scale $\beta_1 = O(Bo)$ it is logical to choose $\xi = x/(BoN)$ as the other independent variable. The equations of energy and radiative transfer valid in various asymptotic regions will now be presented.

Region g: *Optically thin viscous heat-conducting boundary layer*

$$\left.\begin{aligned} \frac{\partial^2 \theta}{\partial \eta^2} + \phi \frac{\partial \theta}{\partial \eta} - 2\xi \frac{d\phi}{d\eta} \frac{\partial \theta}{\partial \xi} &= -\frac{Ec}{4} \left(\frac{d^2 \phi}{d\eta^2} \right)^2 - 2\xi F_g, \\ \frac{\partial^2}{\partial \eta^2} [F_g + 8\theta^4] &= O(Bo/N), \\ \theta(\xi, 0) &= 1/\Delta, \\ \frac{\partial}{\partial \eta} [F_g + 8\theta^4]|_{\eta=0} &= O(Bo/N)^{\frac{1}{2}}, \end{aligned}\right\} \tag{12}$$

where

$$F_g = \frac{F}{\xi^{\frac{1}{2}}} \frac{N^{\frac{1}{2}}}{Bo} \left(\frac{1 - \Delta^4}{\Delta^4} \right), \quad \theta = T/\Delta,$$

$$F = -\frac{\partial q_{Ry}}{\partial \eta}, \quad q_{Ry} = \frac{q'_{Ry}}{\sigma(T'^4_W - T'^4_\infty)},$$

Ec = Eckert number $= u'^2_\infty / C'_p T'_\infty$.

Some explanation regarding these equations and the others which follow are relevant here. A new temperature θ has been defined so that the equations have a simpler form. A subscript is used only on F since it changes definition from region to region, for reasons which will be made clear as and when such changes are made. For example, note that a scaling factor $(N/Bo)^{\frac{1}{2}}$ is introduced in the definition F_g, so that when introduced into the governing energy equation it provides dominant-order interaction between radiation and other modes of energy transfer.

Another important thing to note with respect to (12) is the inclusion of the wall boundary conditions only. No boundary conditions are specified on the other side. These are to be provided by the asymptotic matching conditions.

Region j': Inviscid non-heat-conducting optically finite region

$$\left.\begin{aligned} \frac{\partial\theta}{\partial\xi} &= \tfrac{1}{2}F_{j'}, \\ \frac{\partial^2}{\partial y_{j'}^2}[F_{j'}+8\theta^4] &= 12F_{j'}, \\ \theta(\xi, y_{j'}\to\infty) = 1, \quad F_{j'}(\xi, y_{j'}\to\infty) &= 0, \end{aligned}\right\} \tag{13}$$

where $$y_{j'} = \eta\xi^{\frac{1}{2}}(Bo/N)^{\frac{1}{2}}, \quad F_{j'} = F(N/Bo\xi)^{\frac{1}{2}}(1-\Delta^4)/\Delta^4.$$

These equations can only be made to satisfy the boundary conditions at infinity. The appearance of the absorption term in the equation of transfer provides an attenuation of the radiation leaving the wall and the boundary layer to the zero value at ∞. Being identical to F_g in form, $F_{j'}$ directly matches it asymptotically. The use of $y_{j'}$ as independent variable has the merit of lending a simple form to the energy equation. There is a subtler aspect to it in that the physical distance y rather than the similarity variable η is the proper variable for defining the absorption of radiation leaving the wall and the boundary layer.

Counterparts of the regions g and j' in the large distance limit ($\xi\to\infty$) are the conduction layer g', and the optically thick inviscid non-heat-conducting region j. Remembering that x is scaled now by N/B_0 we introduce a new streamwise variable $\xi_1 = Bo^2\xi$ which is of order unity. With the ideas of matching introduced above in mind, the equations in these regions may now be written down.

Region g': Optically thin conduction layer; no flow to dominant order

$$\left.\begin{aligned} \frac{\partial^2}{\partial\eta_{g'}^2} &= -0{\cdot}44106\,Ec - 2\xi_1 F_{g'}, \\ \frac{\partial^2}{\partial\eta_{g'}^2}[F_{g'}+8\theta^4] &= O(Bo/N), \\ \theta(\xi_1, 0) &= 1/\Delta, \\ \frac{\partial}{\partial\eta_{g'}}[F_{g'}+8\theta^4]\big|_{\eta_{g'}=0} &= O(Bo/N), \end{aligned}\right\} \tag{14}$$

where $$\eta_{g'} = \eta/Bo, \quad F_{g'} = F/Bo(N/Bo\xi_1)^{\frac{1}{2}}.(1-\Delta^4)/\Delta^4.$$

Region j: Optically thick inviscid non-heat conducting region

$$\frac{\partial\theta}{\partial\xi_1} = \frac{F_j}{2}, \tag{15a}$$

$$12F_j - 8\frac{\partial^2\theta^4}{\partial y_j^2} = O(Bo^2/N), \tag{15b}$$

$$\theta(\xi_1, y_j\to\infty) = 1, \quad F_j(\xi_1, y_j\to\infty) = 0,$$

where $$y_j = \eta\xi_1^{\frac{1}{2}}(Bo/N)^{\frac{1}{2}}, \quad F_j = \frac{F}{Bo}\frac{N^{\frac{1}{2}}}{Bo\,\xi_1}(1-\Delta^4)/\Delta^4.$$

Again, the wall boundary conditions are satisfied by (14) and the boundary conditions at ∞ by (15). The choice of y_j as one of the independent variables in region j is natural.

Non-dimensionalizing the conductive wall heat flux with respect to $\sigma(T_W'^4 - T_\infty'^4)$ we have

$$q_{CW} = \left(\frac{Bo}{N}\right)^{\frac{1}{4}} \frac{1}{\xi^{\frac{1}{4}}} \frac{\Delta^3}{2(\Delta^4-1)} \left.\frac{\partial\theta}{\partial\eta}\right|_{\eta=0}. \tag{16a}$$

Using the wall boundary condition on the equation of transfer the radiant part of the wall heat flux is written as

$$q_{RW} = -\left(\frac{N}{Bo}\right)^{\frac{1}{4}} \frac{\chi}{\xi^{\frac{1}{4}}} \left.\frac{F}{12}\right|_{\eta=0}, \tag{16b}$$

where $\chi = 3\epsilon/(2-\epsilon)$ with ϵ the wall emissivity.

4.2. *Solution: linear radiation*

The present treatment of linear radiation has two objectives. We first demonstrate that the concept of radiation slip leads to the same solutions† as the more involved – but more commonly employed – matching procedure. In appendix 1 this equivalence is established for the nonlinear case as well. Secondly, we develop approximate methods of solution for the governing equations – methods we shall later extend to the nonlinear problem. Owing to pressure of space, we shall only be presenting a few highlights of the analysis skipping all the details which can be obtained from Venkateshan (1977).

The governing equations for the linear problem can be derived from equations (12) to (15) by using the following definitions:

$$\Delta = 1+\delta', \quad \theta = 1+\delta \quad \text{with } \delta \text{ and } \quad \delta' \ll 1;$$

$$\Delta^4 \simeq 1+4\delta', \quad \theta^4 \simeq 1+4\delta;$$

$$\theta_l = \left(\theta - \frac{1}{\Delta}\right) \Big/ \left(1 - \frac{1}{\Delta}\right) \simeq 1+\delta/\delta'.$$

Physically these definitions imply that $Ec \ll 1$ (negligible dissipation) and $\Delta \sim 1$ (near isothermal condition).

It is straightforward, though laborious, to construct exact solutions to these equations by the application of Laplace transforms. The solutions for the regions g and j' in the transformed plane are given below:

Outer layer (Region j'):

$$L(\theta_l) = \frac{1}{s} + f_{j'0}(s) \exp\left(-2\left(\frac{3s}{s+16}\right)^{\frac{1}{2}} y_{j'}\right),$$

$$L(F_{j'}) = -\frac{s}{2} f_{j'0}(s) \exp\left(-2\left(\frac{3s}{s+16}\right)^{\frac{1}{2}} y_{j'}\right).$$

Boundary layer (Region g):

A solution in power series of $(Bo/N)^{\frac{1}{4}}$ is sought for the equations in this region. Though we would be interested in the dominant-order solutions only, matching requires a knowledge of the second term in the expansion. The coefficients for the temperature expansion satisfy equations of the form

$$\frac{\partial^2\theta_{gi}}{\partial\eta^2} + \phi\frac{\partial\theta_{gi}}{\partial\eta} - 2\xi\frac{\partial\phi}{\partial\eta}\frac{\partial\theta_{gi}}{\partial\xi} = 8\xi F_{gi}, \quad i = 0, 1, 2, \text{etc.}$$

† Of course, this is true only for leading-order approximations and can not be extended higher-order approximations (see Venkateshan 1977).

The radiative flux functions are given by

$$F_{g0} = f_{g0}(\xi) + \delta\theta_{g0}$$

$$F_{g1} = f_{g1}(\xi) + \chi\eta\xi^{\frac{1}{2}} f_{g0}(\xi) + 8\theta_{g1}.$$

Matching these two sets of solutions in the transformed plane yields the functions $f_{j'0}$ and f_{g0}:

$$\left.\begin{aligned} f_{j'0}(s) &= -\frac{16\chi}{s(s+16)\left(\chi + 2(3^{\frac{1}{2}})\dfrac{s^{\frac{1}{2}}}{s+16}\right)}, \\ L(f_{g0}) &= \frac{-16(3^{\frac{1}{2}})}{s^{\frac{1}{2}}(\chi(s+16)^{\frac{1}{2}} + 2(3^{\frac{1}{2}})s^{\frac{1}{2}})}. \end{aligned}\right\} \tag{17}$$

Equations (17) could also have been derived by the application of the radiation slip boundary condition to the outer-layer equation of transfer. This boundary condition is (Sparrow & Cess 1966)

$$\frac{\partial}{\partial y_{j'}}[F_{j'} - 8\theta_l]|_{y_{j'}=0} = \chi[F_{j'} - 8\theta_l]|_{y_{j'}=0}. \tag{18}$$

Inversion of the transforms (17) is tedious and we will be satisfied here with approximations for large s (small ξ) and small s (large ξ). We shall write down only the solutions for the temperature at the edge of the boundary layer for the case of a black wall ($\chi = 3$):

$$\theta_l|_{y_{j'}=0} \simeq (1 - 7{\cdot}424\xi + 43{\cdot}47\xi^2 - 191\xi^3 + 663{\cdot}9\xi^4 - \ldots) \quad (\xi \text{ small}), \tag{19}$$

$$\theta_l|_{y_{j'}=0} \simeq \frac{1}{(\pi\xi)^{\frac{1}{2}}}\left(\frac{1}{2(3^{\frac{1}{2}})} - \frac{3^{\frac{1}{2}}}{64\xi^2} + \frac{1789(3^{\frac{1}{2}})}{147{\cdot}536\xi^2} + \ldots\right) \quad (\xi \text{ large}). \tag{20}$$

The fact that we are able to provide solutions for small and large ξ as above suggests an approximate method of obtaining these solutions. The starting point for such a solution would obviously be in the neighbourhood of $\xi = 0$ for the outer layer in which we expect only a slight departure from the isothermal condition of the free stream. In this region, the emission term is absent from the equation of transfer and leads to the so-called Raizer limit (Raizer 1957). The solution of such an equation when introduced into the energy equation leads to a departure from the isothermal condition. This in turn provides a non-homogeneous emission term in the equation of transfer. The process can be iterated to obtain the exact solution.

We formalize the above procedure by seeking a series solution to the linearized equations in region j':

$$\theta_l = 1 + \left[\sum_{n=0}^{\infty} \theta_{ln}(\xi)\, y_{j'}^n\right] \exp(-2(3^{\frac{1}{2}})y_{j'}),$$

$$F_{j'} = 1 - \frac{1}{2}\left[\sum_{n=0}^{\infty} \frac{d\theta_{ln}}{d\xi}\, y_{j'}^n\right] \exp(-2(3^{\frac{1}{2}})\, y_{j'}). \tag{21}$$

Various approximations to the solution can be constructed by truncating the series to various orders. We shall not reproduce these approximations here (but later indi-

cate some results graphically to give an idea about the usefulness of the approximation), but only give the exact slip temperature obtained by the procedure:

$$L(\theta_l)|_{y_{j'}=0} = \frac{1}{s} - \frac{16\chi}{\chi+2(3^{\frac{1}{2}})} \frac{1}{s(s+16)} \frac{1}{\left[1 - \frac{16(3^{\frac{1}{2}})}{(\chi+2(3^{\frac{1}{2}}))\,(s+16)\,H(s)}\right]}, \tag{22}$$

where

$$H(s) = 1 - \frac{(8s+16)}{1-} \frac{(4/s+16)}{1-} \frac{(4/s+16)}{1-} \tag{23}$$

$$= (s/s+16)^{\frac{1}{2}}.$$

In the above we have used the standard notation of the continued fraction. The last part of the equations follows from theorems on continued fractions (Smith 1957) and is strictly valid for $s \gg 1$. We have again used Laplace transforms and the wall slip boundary condition [equation (17)]. Equation (23) is of course the same as the one that was obtained earlier by the exact procedure.

The equations in the boundary layer are of the same form mentioned earlier and will not be repeated here. It is a partial differential equation which can be solved by the local similarity approximation (see appendix B for justification). The approximation leads to a two-point boundary-value problem to be solved numerically.

Turning now to the regions g' and j, we note that they both have the form of the simple heat conduction equation. The slip boundary condition has now the form

$$\left.\frac{\partial\theta_l}{\partial y_j}\right|_{y_j=0} = \chi\theta_l|_{y_j=0}. \tag{24}$$

The solutions can again be obtained very simply by Laplace transforms and are:
Slip temperature:

$$\theta_l|_{y_j=0} = \exp\left(\frac{4\chi^2\xi_1}{3}\right) \operatorname{erfc}\left(\frac{2\chi\xi_1^{\frac{1}{2}}}{3^{\frac{1}{2}}}\right). \tag{25}$$

Conduction layer:

$$\theta_l = \theta_l|_{y_j=0}[1 - \exp(-8\eta_{g'}\xi_1^{\frac{1}{2}}],$$

$$F_{g'} = 8\xi_1^{\frac{1}{2}}[\theta_l - \theta_l|_{y_j=0}]. \tag{26}$$

We end this section by presenting heat flux results obtained by substituting the relevant quantities into (16). Small ξ boundary layer:

$$q_{RW} = -\frac{\chi}{12} f_{g0}, \quad Q_{CW} = \frac{1}{8\xi^{\frac{1}{2}}} \left.\frac{d\theta_l}{d\eta}\right|_{\eta=0}.$$

Large ξ conduction layer:

$$q_{RW} = -\frac{2\chi}{3}\theta_l|_{y_j=0}, \quad Q_{CW} = \theta_l|_{y_j=0}, \tag{27}$$

where

$$Q_{CW} = \left(\frac{N}{Bo}\right)^{\frac{1}{2}} \cdot q_{CW}.$$

4.3. *Solution: nonlinear radiation*

We first present the approximate solution obtained by extending the development in the previous section. Only the first approximation results have been calculated. We also obtain an exact numerical solution which serves as a check against the approximate solution and also provides a solution for $\xi = O(1)$.

As in the previous section, we start with the solution in region j' [equation (13)]. We use the radiation slip method and the slip boundary condition is expressed for this case as:

$$\frac{\partial}{\partial y_{j'}}[F_{j'}+8\Theta^4]|_{y_{j'}=0} = \chi\left[F_{j'}+8\left(\Theta^4-\frac{1}{\Delta^4}\right)\right]\Big|_{y_{j'}=0}. \tag{28}$$

In analogy with the expansions (21), we seek a solution of the form

$$\Theta = 1+\sum_{m=1}^{\infty}\sum_{n=0}^{\infty}\Theta_{mn}(\xi)\,y_{j'}^{n}\exp\left(-2(3^{\frac{1}{2}})\,m y_{j'}\right). \tag{29}$$

(Note that for linear radiation we do not have a double series.) By first approximation, we mean

$$[\Theta]_1 \simeq 1+\Theta_{10}\exp\left(-2(3^{\frac{1}{2}})\,y_{j'}\right)+\Theta_{20}\exp\left(-4(3^{\frac{1}{2}})\,y_{j'}\right) + \Theta_{30}\exp\left(-6(3^{\frac{1}{2}})\,y_{j'}\right)+\Theta_{40}\exp\left(-8(3^{\frac{1}{2}})\,y_{j'}\right). \tag{30}$$

Introducing these into the equation of transfer, we can obtain an explicit solution as follows:

$$F_{j'} = (f_{j'0}+8\Theta_{10})\exp\left(-2(3^{\frac{1}{2}})\,y_{j'}\right)+32(3^{\frac{1}{2}})\,\Theta_{10}y_{j'}\exp\left(-2(3^{\frac{1}{2}})\,y_{j'}\right) - 64\Theta_{10}^2\exp\left(-4(3^{\frac{1}{2}})\,y_{j'}\right)-36\Theta_{10}^3\exp\left(-6(3^{\frac{1}{2}})\,y_{j'}\right)-\tfrac{128}{15}\,\Theta_{10}^4\exp\left(-8(3^{\frac{1}{2}})\,y_{j'}\right). \tag{31}$$

$f_{j'0}$ is determined by the slip boundary condition as

$$f_{j'0} = \frac{1}{\chi+2(3^{\frac{1}{2}})}\Big[-8\chi\left(1-\frac{1}{\Delta^4}\right)-8(5\chi+6(3^{\frac{1}{2}})\,\Theta_{10}+16(\chi+4(3^{\frac{1}{2}}))\,\Theta_{10}^2 + 4(\chi+6(3^{\frac{1}{2}}))\,\Theta_{10}^3+\tfrac{8}{15}(\chi+8(3^{\frac{1}{2}}))\,\Theta_{10}^4\Big]. \tag{32}$$

In the above equations, the cross-product terms that arise from taking the fourth power of $[\Theta]_1$ have all been ignored.

Using (31) and (32) in the energy equation, the following equations result:

$$\frac{d\Theta_{10}}{d\xi} = \Big[-4\chi\left(1-\frac{1}{\Delta^4}\right)-16(\chi+3^{\frac{1}{2}})\,\Theta_{10}+8(\chi+4(3^{\frac{1}{2}}))\,\Theta_{10}^2 + 2(\chi+6(3^{\frac{1}{2}}))\,\Theta_{10}^3+\tfrac{4}{15}(\chi+8(3^{\frac{1}{2}}))\,\Theta_{10}^4\Big]\Big/(\chi+2(3^{\frac{1}{2}}));$$

$$\frac{d\Theta_{20}}{d\xi} = -32\Theta_{10}^2;\quad \frac{d\Theta_{30}}{d\xi} = -18\Theta_{10}^3;\quad \frac{d\Theta_{40}}{d\xi} = -\tfrac{64}{15}\,\Theta_{10}^4. \tag{33}$$

All these equations have zero initial conditions. These equations of course need a numerical solution, which will lead to the temperature at the edge of the boundary layer.

A completely numerical solution for the equations in region j' have been obtained by the Crank–Nicholson scheme (Ralston 1965). The convergence of the implicit scheme is accelerated by an iteration scheme using quasi-linearization (Roberts & Shipman 1972). The linear tridiagonal matrix that results from the above procedure is solved by the Thomas algorithm (Ralston 1965). For every iteration on this system of equations, an iteration is performed on the slip boundary condition, again using quasi-linearization.

In the boundary layer [equation (12)] the equation of transfer can be directly integrated to yield

$$F_g + 8\Theta^4 = f_{g0}(\xi), \tag{34}$$

where f_{g0} is obtained by matching with the outer solution as

$$f_{g0}(\xi) = 8\Theta|^4_{y_j=0} + 2\frac{d\Theta_{10}}{d\xi}. \tag{35}$$

These when substituted into the energy equation lead to the following partial differential equation which is solved by the local similarity approximation:

$$\frac{\partial^2\Theta}{\partial\eta^2} + \phi\frac{\partial\Theta}{\partial\eta} - 2\xi\frac{\partial\phi}{\partial\eta}\frac{\partial\Theta}{\partial\xi} = -\frac{Ec}{4}\left(\frac{d^2\phi}{d\eta^2}\right)^2 - 2\xi\left\{8(\Theta|^4_{y_j=0} - \Theta^4) + 2\frac{d\Theta_{10}}{d\xi}\right\},$$

$$\Theta(\xi, 0) = \frac{1}{\Delta} \quad \text{and} \quad \Theta(\xi, \eta \to \infty) = \Theta|_{y_{j'}=0}. \tag{36}$$

To round off this treatment of the nonlinear case, we present some salient features of the solutions in regions j and g'. Equations (15a) and (15b) are combined to yield

$$3\frac{\partial\Theta}{\partial\xi} = \frac{\partial^2\Theta^4}{\partial y_j^2}, \tag{37}$$

with the slip boundary condition

$$\left.\frac{\partial\Theta^4}{\partial y_j}\right|_{y_j=0} = \chi\left.\left(\Theta^4 - \frac{1}{\Delta^4}\right)\right|_{y_j=0},$$

and the condition at infinity $\Theta|_{y_j\to\infty} = 1$. (38)

In the conduction layer, the equation of transfer is readily integrated to yield

$$F_{g'} = f_{g'_0} - 8\Theta^4. \tag{39}$$

The energy equation, after multiplying by $2(\partial\Theta/\partial\eta_{g'})$ can be integrated once resulting in

$$\left(\frac{\partial\Theta}{\partial\eta_{g'}}\right)^2 = -(0{\cdot}8821\,Ec + 4\xi_1 f_{g'_0})\,\Theta + 32\xi_1\frac{\Theta^5}{5} + f_{g'_1}. \tag{40}$$

$f_{g'_1}$ is determined by the condition $(\partial\Theta/\partial\eta_{g'}) \to 0$ as $\eta_{g'} \to \infty$ while $f_{g'_0}$ is obtained by matching with the solution of equation of transfer [equation (15b)]. These result in

$$f_{g'_1} = -\frac{32\xi_1\Theta|^5_{y_j=0}}{5} + (0{\cdot}8821Ec + 4\xi_1 f_{g'_0})\,\Theta|_{y_j=0}, \tag{41}$$

and

$$f_{g'_0} = 8\Theta|^4_{y_j=0} - 2\left.\frac{\partial\Theta}{\partial\xi_1}\right|_{y_j=0}. \tag{42}$$

Equation (40) has the initial condition $\Theta(\xi_1, 0) = 1/\Delta$. In contrast with the linear problem, the temperature field in the conduction layer is non-similar.

5. Results and discussion

We present here a few results to demonstrate the physical aspects of the radiation interaction and to allow certain comparisons with some earlier work to establish the validity of the procedures adopted in this work. The two-point boundary-value prob-

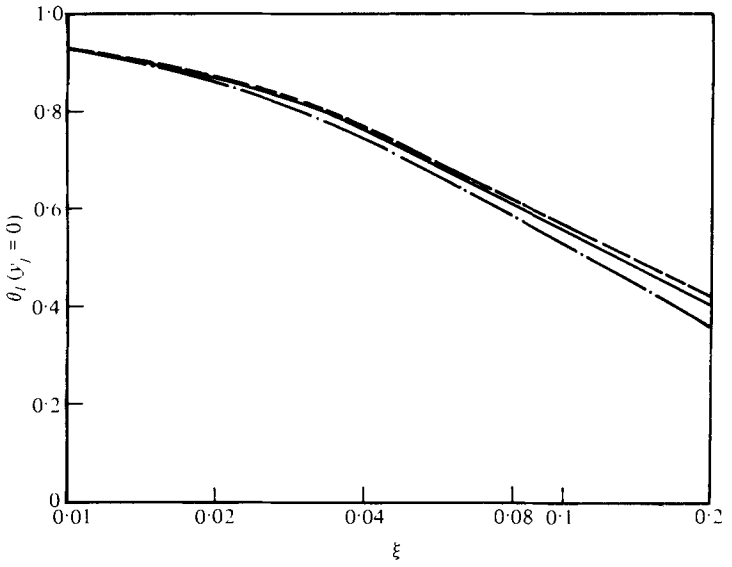

FIGURE 3. Slip temperature in the boundary-layer region. – – –, first approximation; ——, fourth approximation; – · – · –, Cess solution. $\Delta \sim 1$. $\chi = 3$.

lems in the boundary layer have been solved by the Gill method (Ralston & Wilf 1960). For the nonlinear equation quasi-linearization is resorted to at each iteration step.

5.1. *Linear radiation*

Figure 3 depicts the wall slip temperature in the boundary layer region g. For the range of ξ considered, the first approximation [$n = 1$ in equation (21)] is a very good description being very close to the fourth approximation, which is indistinguishable from the exact solution [equation (19)]. The comparison of the present solution with those of Cess (1966)† and Taitel (1969) (these two solutions coincide with one another) shows that the present results slightly overestimate the wall slip. In the conduction layer, all the results (figure 4) – the result of equation (20), the optically thick result [equation (26)], the Cess and Taitel results – coincide with one another for $\xi > 1$. These demonstrate that the differential approximation provides an adequate description of the radiation field for the entire range of optical thicknesses for the present problem.

The temperature profiles in the boundary layer for different values of ξ are presented in figure 5. As ξ increases, there is an increase in the wall temperature gradient with a general flattening of the profile in the outer regions, thus anticipating the presence of the conduction layer for large values of ξ. This clearly shows that as we proceed downstream along the plate, the radiation process begins to dominate the convective process, a fact that was earlier alluded to in the asymptotic analysis. The similarity temperature profile in the conduction layer is shown in figure 6.

Figures 7 and 8 present heat flux results in the boundary-layer region and the

† Cess uses an exponential kernel solution by the following approximations:

$$E_1(\tau) \sim 2\exp(-2\tau), \quad E_2(\tau) \sim \exp(-2\tau).$$

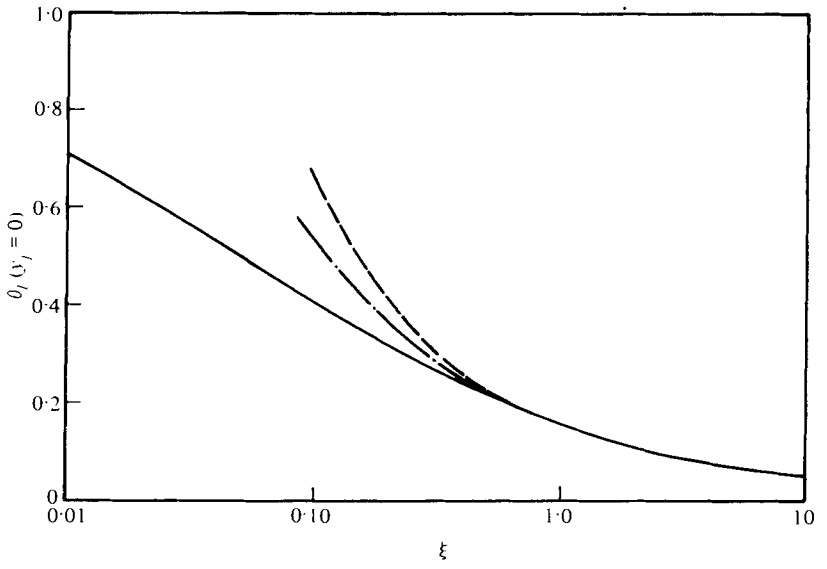

FIGURE 4. Slip temperature in the conduction-layer region. ——, solution of expression (25); – – –, 'exact' solution in inverse powers of $\xi_1^{\frac{1}{2}}$; – · – · – Cess solution. $\Delta \sim 1$. $\chi = 3$.

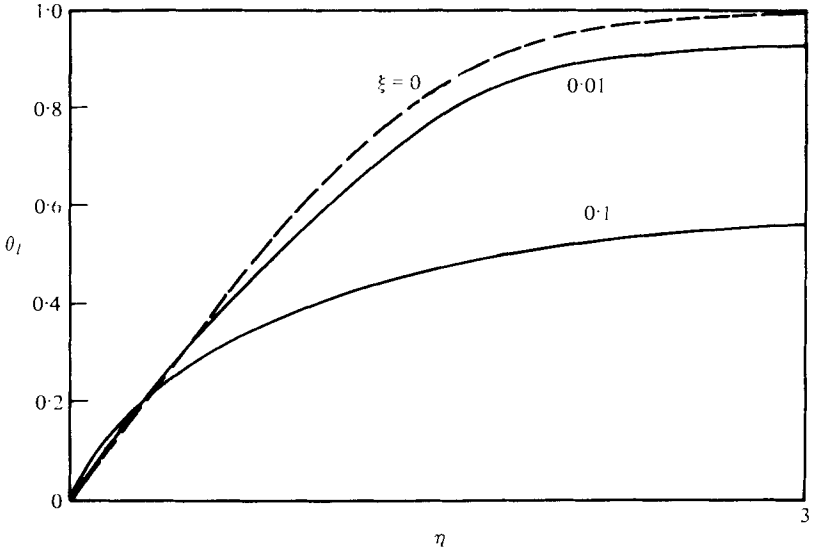

FIGURE 5. Boundary-layer temperature profile development. – – –, no radiation; ——, with radiation. $\Delta \sim 1$. $\chi = 3$.

conduction layer respectively. The normalization employed makes the conductive and radiative wall heat fluxes of the same order of magnitude. We shall make some comments on the actual values at a later stage. An examination of these results indicates that (*a*) the radiative interaction enhances the conductive heat flux by as much as 80 % when compared with the non-interaction result; and (*b*) there is a marked reduction in the radiative flux with increasing ξ.

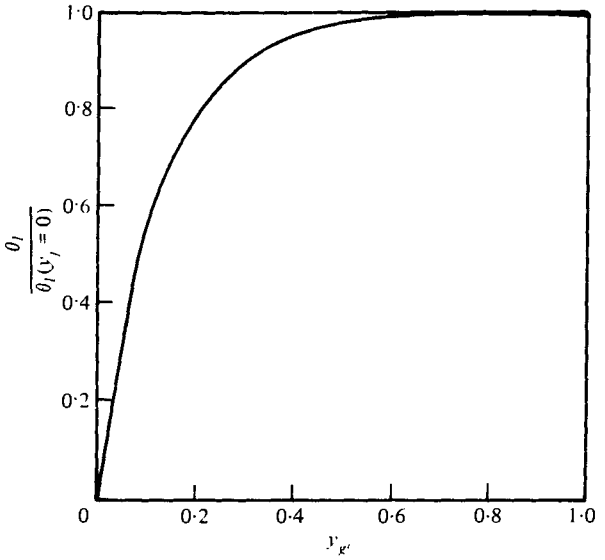

FIGURE 6. Conduction-layer temperature profile. $\Delta \sim 1$. $\chi = 3$.

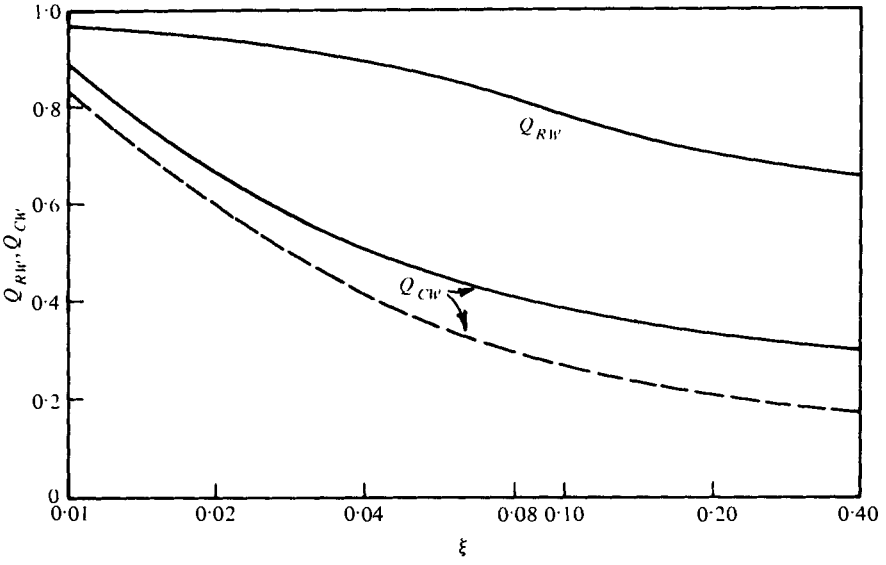

FIGURE 7. Wall heat flux in the boundary-layer region.
– – –, no interaction. $\Delta \sim 1$. $\chi = 3$.

5.2. *Nonlinear results*

The parameters Δ and Ec enter into the consideration of the nonlinear problem. In particular, we will treat the cases of $\Delta < 1$ (hot wall) and $\Delta > 1$ (cold wall) separately.

Figure 9 depicts the wall slip temperature for a cold wall calculated by various methods – the approximate method, the finite difference solution to the full equation of transfer, the optically thick outer equation and a linearized outer field solution for small ξ. The results show that the approximate solution agrees with the numerical

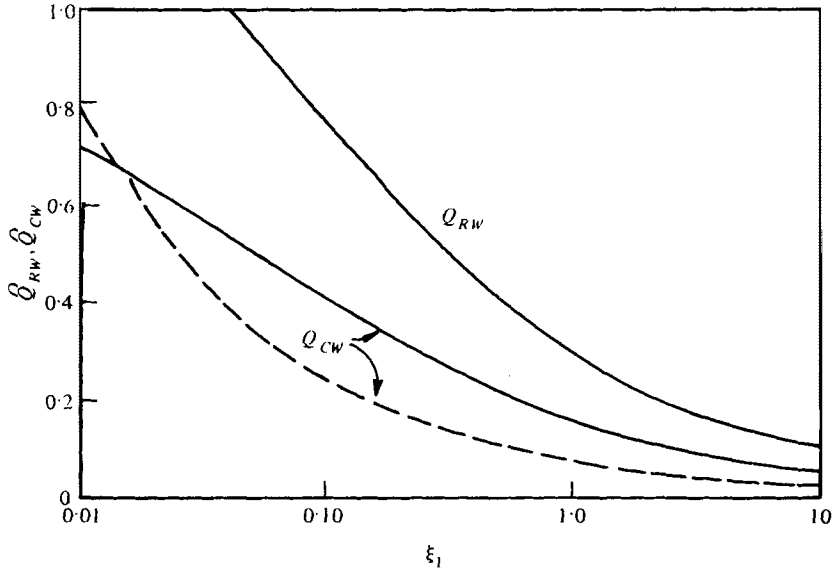

FIGURE 8. Wall heat flux in the conduction-layer region. ---, no interaction. $\Delta \sim 1$. $\chi = 3$.

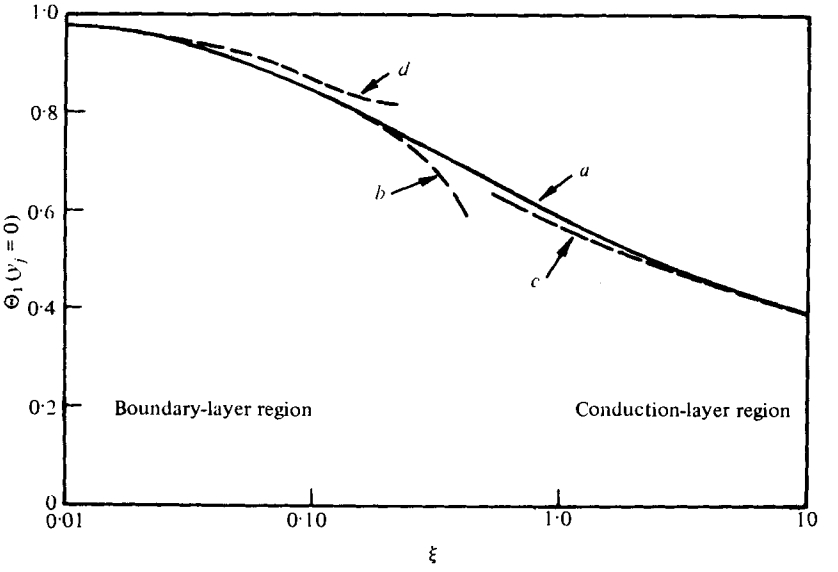

FIGURE 9. Slip temperature comparisons. Cold wall. $\Delta = 5$. $\chi = 3$. *a*, complete equation of transfer (exact); *b*, small ξ approximate solution; *c*, optically thick solution; *d*, linearized radiation.

solution to within about 5 % up to $\xi = 0{\cdot}3$. The linearized outer field solution is itself an excellent approximation up to $\xi = 0{\cdot}1$. The latter is not surprising if we note that in the neighbourhood of $\xi = 0$, the departure from the isothermal condition in the outer field is very slight and linearization is possible under such conditions. In the conduction-layer region both the exact and the optically thick result coincide. The

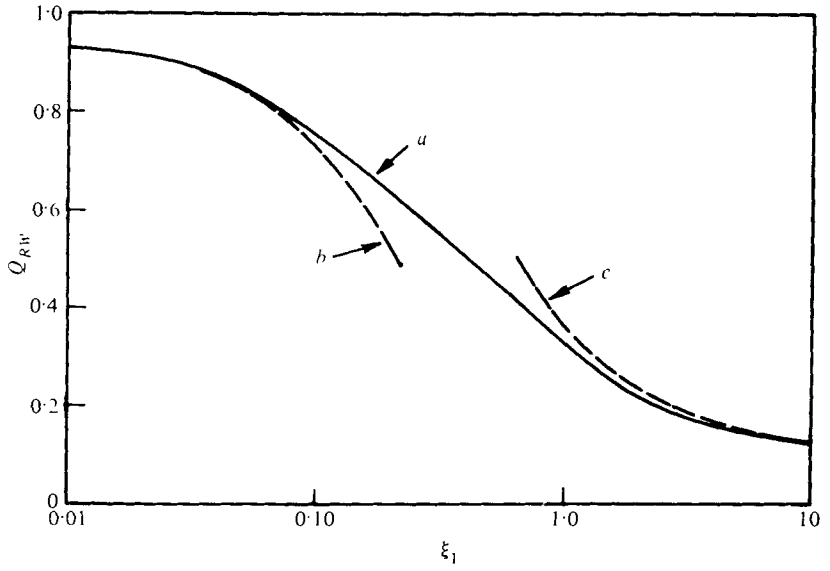

FIGURE 10. Radiant wall heat flux. Cold wall. $\Delta = 5$. $\chi = 3$. *a*, complete equation of transfer (exact); *b*, small ξ approximate solution; *c*, optically thick solution.

exact solution, apart from validating the approximate solution, bridges the gap between the small ξ and large ξ solutions.

For the conditions of figure 9, the radiative wall heat flux is plotted in figure 10. It is to be noted that this flux can be deduced from the outer solution. The flux results from the approximate solution agree well with the exact solution up to about $\xi = 0{\cdot}5$ and in the conduction-layer region the agreement of the optically thick solution with the exact solution is very good.

In figure 11 we show plots of slip temperature and radiant heat flux for a hot wall ($\Delta = 0{\cdot}5$). In contrast with the cold wall solution where slow cooling is observed, there is a marked heating of the gas at smaller values of ξ.

We now turn to the boundary-layer temperature profiles. In general, the pattern of behaviour is similar to the one we observed for linear radiation. For a cold wall with negligible dissipation figure 12 shows the development of the temperature profile in the boundary layer. The non-interacting self-similar solution at $\xi = 0$ is transformed with the inclusion of radiative interaction to the non-similar conduction-layer profile at $\xi = 10$. The effect of dissipation ($M = 2$) is to more than double the wall temperature gradient (figure 13). For this Mach number, we observe no temperature overshoot when radiation is absent; however, inclusion of radiation results in an overshoot over the local slip temperature. For $\xi = 0{\cdot}2$ a change in slope of the temperature profile occurs at $\eta = 1{\cdot}3$.

At this stage two interesting comparisons are made. Firstly, we compare the present results with weak interaction ($Bo > 1$) profile obtained by linearizing the temperature field with respect to the one with no radiation (this work is treated elsewhere, Venkateshan 1977). Figure 14 shows that the weak interaction theory provides an excellent approximation for the wall temperature gradient for values of ξ as large as $0{\cdot}1$. This is the counterpart of linearized outer field, where temperature was linearized

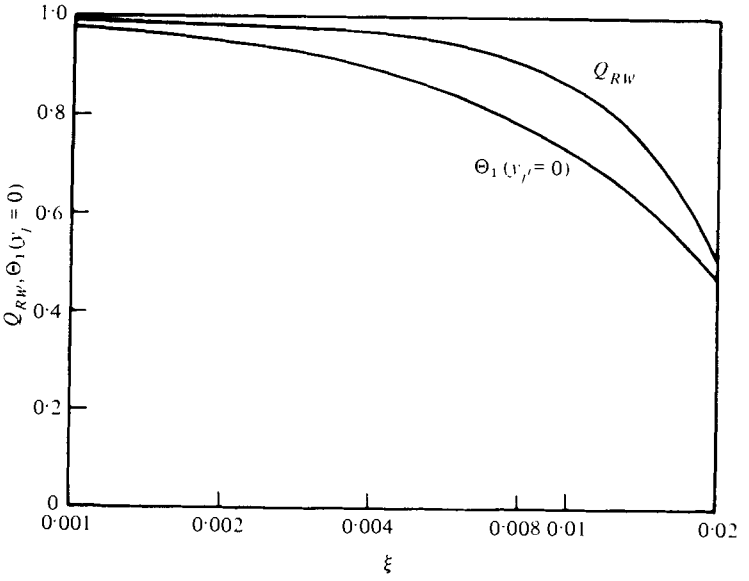

FIGURE 11. Slip temperature and radiant wall heat flux. Hot wall. $\Delta = 0{\cdot}5$. $\chi = 3$.

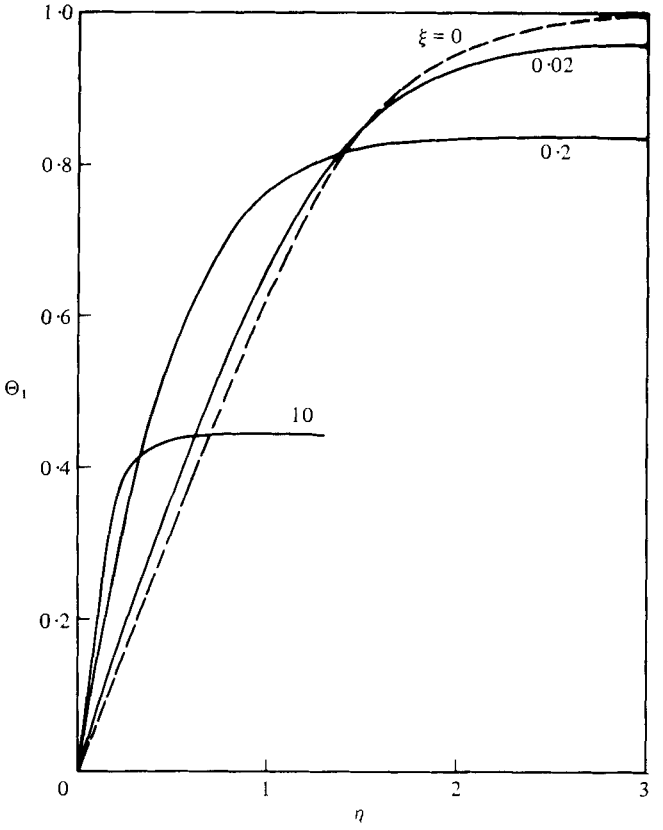

FIGURE 12. Boundary-layer temperature profile development. ---, no radiation; ——, with radiation. $\Delta = 5$. $Ec = 0$. $\chi = 3$.

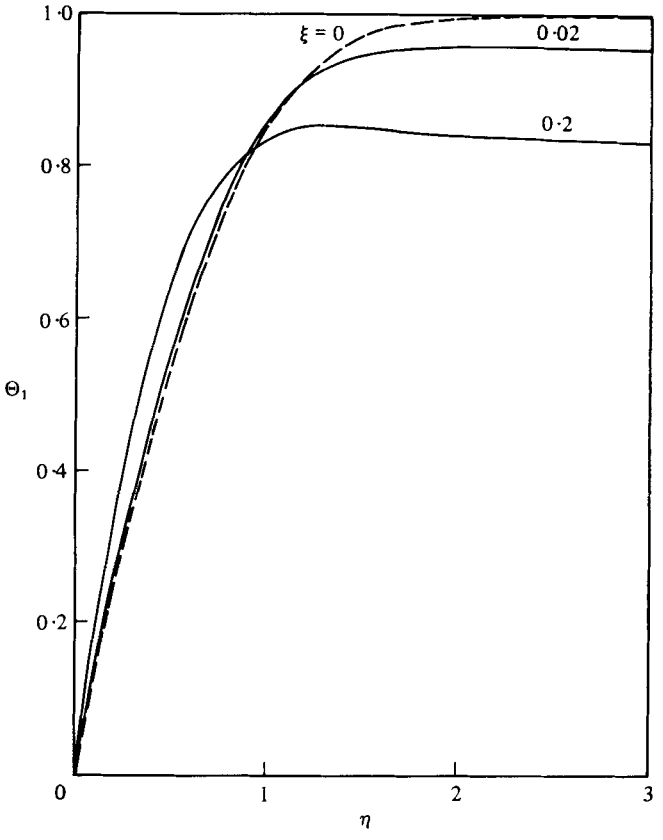

FIGURE 13. Boundary-layer temperature profile development. – – –, no radiation; ——, with radiation. $\Delta = 5$. $Ec = 1{\cdot}6$ ($M = 2$). $\chi = 3$.

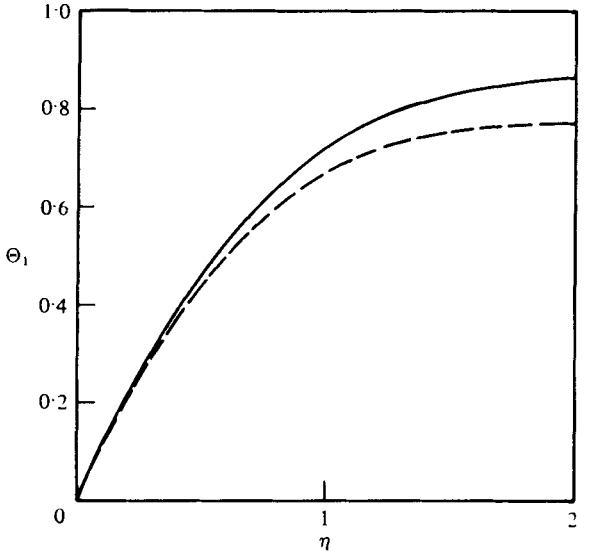

FIGURE 14. Boundary-layer temperature profile: comparison of weak and strong interaction results. – – –, weak interaction; ——, strong interaction. $\Delta = 5$. $\xi = 0{\cdot}1$, $Ec = 0$. $\chi = 3$.

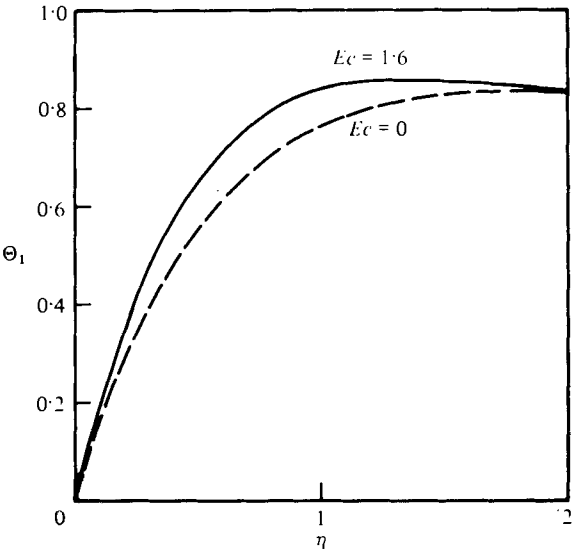

FIGURE 15. Effect of dissipation on boundary-layer temperature profile. ---, no dissipation; ——, with dissipation. $\Delta = 5$. $\xi = 0{\cdot}2$. $\chi = 3$.

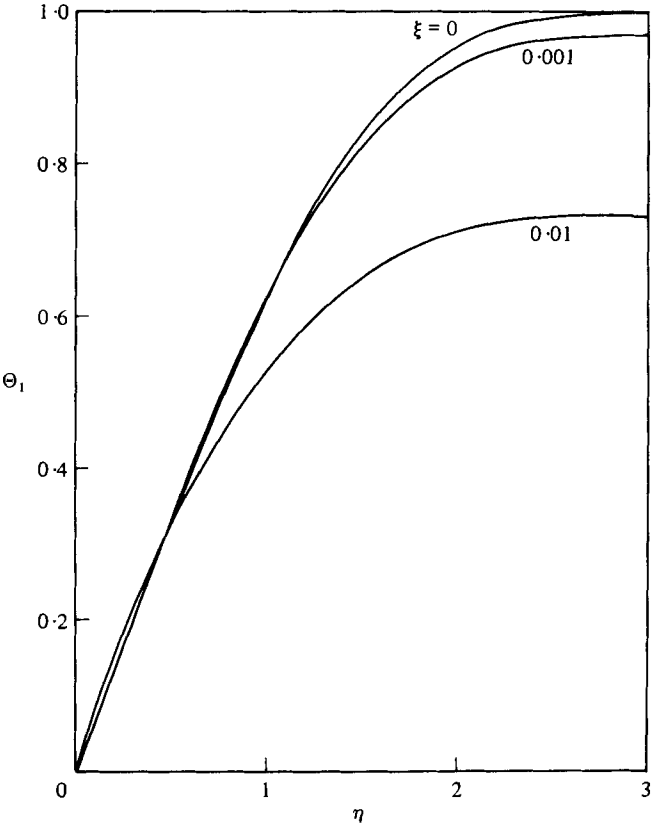

FIGURE 16. Boundary-layer temperature profiles. Hot wall. $\Delta = 0{\cdot}5$. $Ec = 0$. $\chi = 3$.

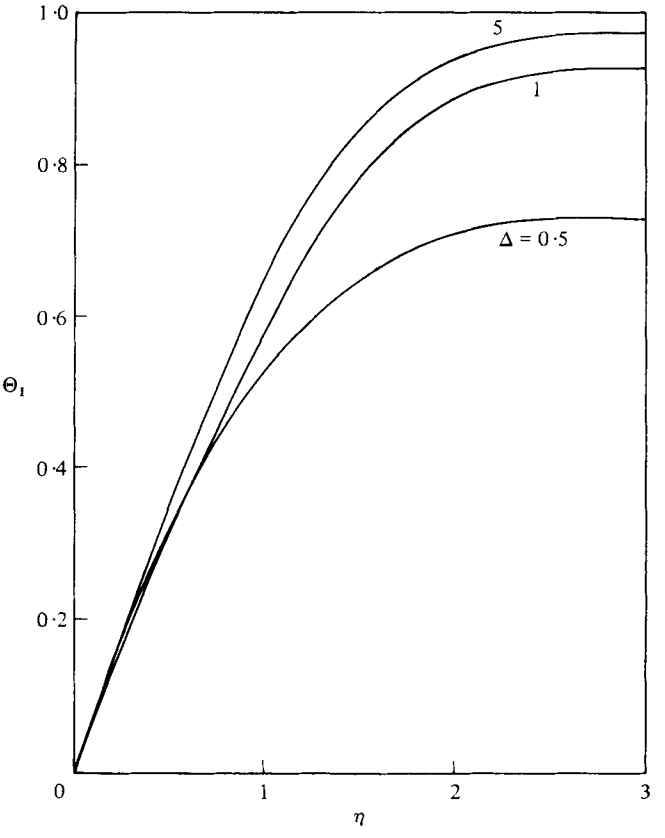

FIGURE 17. Effect of Δ on boundary-layer temperature profile. $\xi = 0{\cdot}01$. $Ec = 0$. $\chi = 3$.

with respect to the free-stream temperature which showed good agreement with the exact solution up to $\xi = 0{\cdot}1$. This shows that the linear radiation results have more use than one would expect. As an excellent approximation we could use linearized outer and inner fields to solve the problem, linearization being carried out as mentioned above. The second comparison is between the temperature profiles with and without dissipation. Figure 15 shows that dissipation increases the temperature everywhere, including the wall temperature gradient.

While the nonlinear hot wall results show a large temperature slip, the effect on the wall gradient is not as marked (figure 16). This is consistent with our observation above that weak and strong interaction theories are equally capable of predicting the wall temperature gradient in this range of ξ. The profiles of figure 17 reinforce this point. For $\xi = 0{\cdot}01$ the profiles for a hot wall ($\Delta = 0{\cdot}5$), linearized profile ($\Delta \sim 1$) and the cold wall ($\Delta = 5$) show that though the wall slip goes through a large variation ($0{\cdot}04$ for $\Delta = 5$, $0{\cdot}07$ for $\Delta \sim 1$, and $0{\cdot}27$ for $\Delta = 0{\cdot}5$) the temperature gradient remains almost constant ($0{\cdot}738$ for $\Delta = 5$, $0{\cdot}702$ for $\Delta \sim 1$ and $0{\cdot}7$ for $\Delta = 0{\cdot}5$).

Figure 18 shows the developing conduction-layer profile normalized with respect to the local slip value for a cold wall. The figure also includes the similar solution of the linearized problem for comparison. Though with respect to $y_{g'}$, there is a decrease in the wall temperature gradient (with increasing ξ_1), with respect to η it always shows an increase (see figure 12).

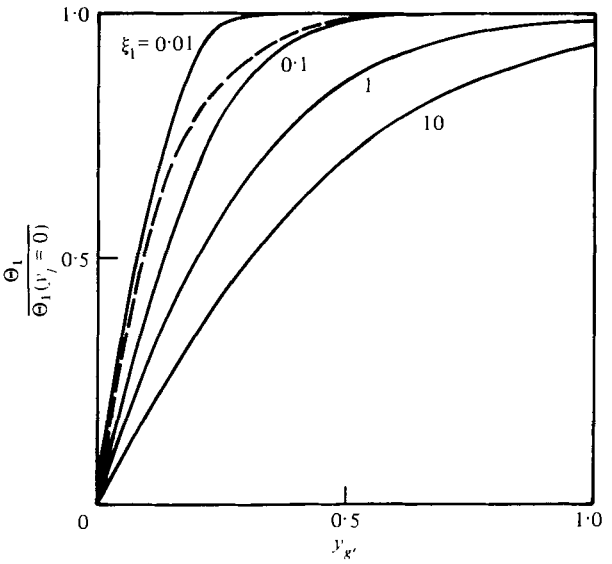

FIGURE 18. Developing conduction-layer profile. – – –, linear radiation. $\Delta = 5$. $Ec = 0$. $\chi = 3$.

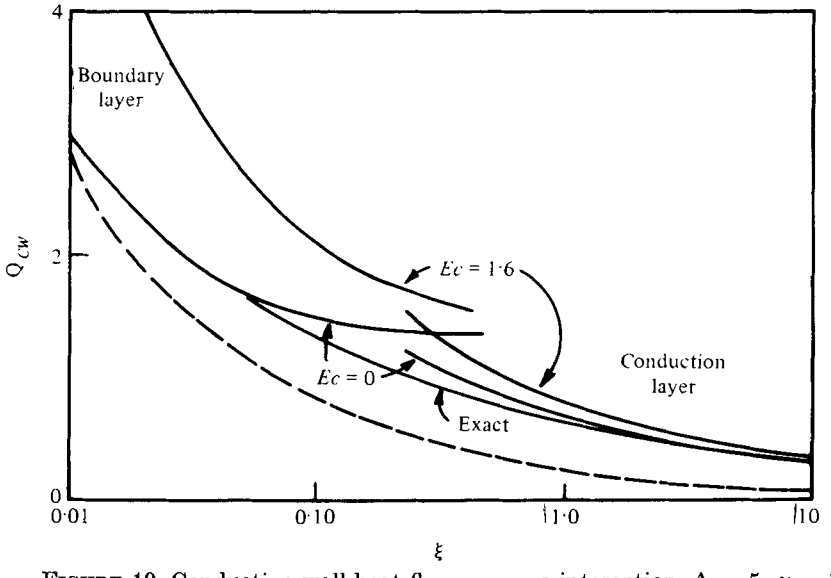

FIGURE 19. Conductive wall heat flux. – – –, no interaction. $\Delta = 5$. $\chi = 3$.

To complete the picture of wall heat transfer, we now present the conductive wall heat flux (figure 19). The effect of interaction is seen to enhance the conductive heat flux by as much as 80 %. Though dissipation has a marked influence in the boundary-layer region, it has a very minor effect in the conduction layer. This is as it should be since the conduction layer strikes a balance between only radiation and conduction.

We sum up our results by presenting the influence of the Boltzmann number (which has a major role according to the asymptotic analysis of §3) on the radiant and conductive wall heat fluxes. Figure 20 shows the radiant wall heat flux for $\Delta = 0{\cdot}5$ (hot

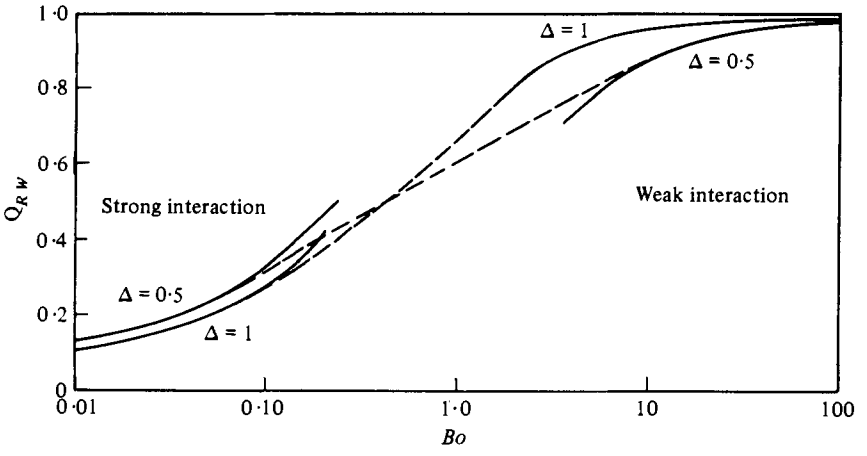

FIGURE 20. Effect of the Boltzmann number on radiant wall heat flux. $x = 10^5$. $N = 10^6$. $\chi = 3$.

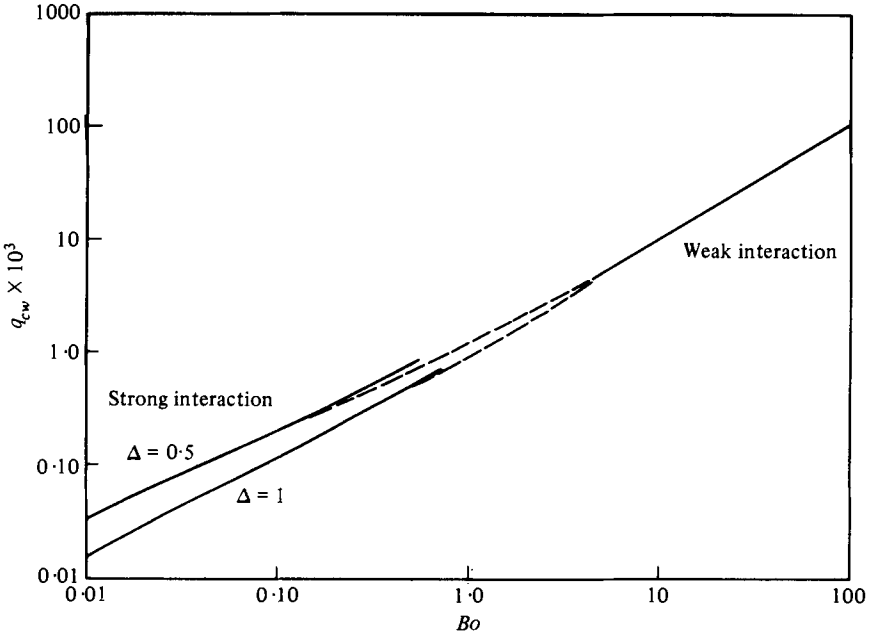

FIGURE 21. Effect of the Boltzmann number on conductive wall heat flux. $x = 10^5$. $N = 10^6$. $\chi = 3$.

wall) and the linearized solution ($\Delta \sim 1$). The strong and weak interaction results form asymptotic descriptions along the Boltzmann number axis. It is interesting to note that the linear solution is less affected by interaction for large Boltzmann number and more affected for small Boltzmann number as compared with the nonlinear solution. The conductive wall heat flux (figure 21) changes through several orders of magnitude as the linear result is lower than the nonlinear result up to about $Bo = 5$ after which both coincide.

A significant result emerges from a careful study of figures 20 and 21. While we can

neglect conductive heat flux altogether at $Bo = 0{\cdot}01$, we may not neglect radiative heat transfer even at $Bo = 100$ (it does not matter whether we use the linear or non-linear result). In fact at $Bo = 100$ conductive heat flux is only 10 % of the radiative heat flux. Note that this follows from equation (12) where the radiative flux term is multiplied by x/Bo (where x is the Reynolds number) while the coefficient of conductive flux is unity. This has an important implication for the solution procedure we need to adopt for a practical problem. For the strong interaction problem (the problem that is considered in this paper), we need only solve the outer equations with the slip boundary condition to obtain the total wall flux to a good approximation. For the weak interaction problem, we can solve the energy equation ignoring the radiation term in it. This solution can be used to calculate both the radiative and conductive heat fluxes.

6. Concluding remarks

A detailed description of radiative interactions in laminar boundary layers by way of asymptotic analysis and supporting solutions for large N and small Bo has been presented in the preceeding sections. The introduction of what we call non-optimal regions is a significant feature of the present work. These regions, although not essential in the Kruskal sense for the construction of solutions to the problem, are powerful aids in visualizing the physics of the problem. Also, solutions based on such regions are more than adequate for many practical problems.

To sum up the physics of the problem, the outer inviscid region and the wall layer behave in distinctly different ways. The outer field starts out with isothermal conditions near the leading edge, gradually absorbs the radiation leaving the wall and the process is described by the Raizer limit corresponding to an absorbing, but non-emitting gas (this is one of the non-optimal regions, we mentioned earlier). The process in due course induces a temperature non-uniformity so that emission becomes important. Far downstream of this region (and of course at large distances from the wall, large compared with the photon mean free path) both emission and absorption are equally important and the medium acquires an optically thick character. It is to be remembered, however, that this optically thick medium is representative of the growth of the physical dimensions of the region of temperature non-uniformity induced by the radiation–convection interaction. Measured in boundary-layer variables, these dimensions are very large indeed and as such the temperature non-uniformity mentioned above will not result in any significant conductive heat flux.

The wall layer close to the leading edge is convection dominant. As the flow proceeds downstream the effect of radiation gains importance with a consequent increase in the wall temperature gradient and a general flattening of the temperature profile away from the wall. Far downstream, this flattening becomes so predominant that in the radiation dominant limit, the viscous boundary layer is isothermal to the leading order. However, there is still a region of small optical thickness close to the wall where owing to the high temperature gradients, conduction plays a role equally important to that of radiation.

The following interesting observation emerges from the above discussion. In the weak radiation limit the optically thin approximation cannot form a uniform approximation to the radiation field, and hence requires an outer field where radiation acts

over a distance of the order of a photon mean free path. In the strong radiation limit the optically thick approximation cannot form a uniform approximation to the radiation field and hence requires a wall layer where the radiation field is optically thin.

These conclusions lead to a few comparisons. For very small ξ there appears to be a formal similarity between the present solution and the modified differential approximation result (Olfe 1967; Koch 1972). Emanuel (1968, 1970) shows that the optically thick approximation cannot form a uniform description of the radiation field, breaking down close to a solid boundary, where a thermal wall layer is observed even in the absence of other modes of energy transport. The radiation conduction interaction problem of Lick (1963) shows the presence of optically thin conduction boundary layers close to the boundaries where the optically thick approximation breaks down. These wall layers are similar to the conduction layer in the present work.

Appendix A. Equivalence of the radiation slip method and the matched asymptotic expansion solution for the nonlinear problem

Seeking solutions of the form

$$\Theta = \Theta_0 + \left(\frac{Bo}{N}\right)^{\frac{1}{2}} \Theta_1 + \ldots,$$

$$F_g = F_{g0} + \left(\frac{Bo}{N}\right)^{\frac{1}{2}} F_{g1} + \ldots, \tag{A 1}$$

in the boundary layer g, the governing equations (12) yield

$$\frac{\partial^2 \Theta_0}{\partial \eta^2} + \phi \frac{\partial \Theta_0}{\partial \eta} - 2\xi \frac{\partial \phi}{\partial \eta} \frac{\partial \Theta_0}{\partial \xi} = -\frac{Ec}{4} \left(\frac{\partial^2 \phi}{\partial \eta^2}\right)^2 - 2\xi F_{g0},$$

$$\frac{\partial^2 \Theta_1}{\partial \eta^2} + \phi \frac{\partial \Theta_1}{\partial \eta} - 2\xi \frac{\partial \phi}{\partial \eta} \frac{\partial \Theta_1}{\partial \xi} = -2\xi F_{g1},$$

$$F_{g0} = f_{g0}(\xi) - 8\Theta_0^4,$$

$$F_{g1} = f_{g1}(\xi) + \chi \eta \xi^{\frac{1}{2}} \left(f_{g0}(\xi) - \frac{8}{\Delta^4}\right) - 32\Theta_0^3 \Theta_1, \tag{A 2}$$

where the wall boundary conditions have been satisfied. The outer limit of the boundary-layer solutions can be written as

$$\Theta|_{\eta\to\infty} \sim \Theta_0|_{\eta\to\infty} + \left(\frac{Bo}{N}\right)^{\frac{1}{2}} \Theta_1|_{\eta\to\infty} + \ldots,$$

$$F_g|_{\eta\to\infty} \sim f_{g0} - 8\Theta_0^4|_{\eta\to\infty} + \left(\frac{Bo}{N}\right)^{\frac{1}{2}} \left[f_{g1} + \chi\eta\xi^{\frac{1}{2}} \left(f_{g0} - \frac{8}{\Delta^4}\right) - 32\Theta_0^3 \Theta_1 |_{\eta\to\infty}\right]. \tag{A 3}$$

Asymptotic matching with the outer solution in the region j' for $y_{j'} \to 0$ will require that $\Theta_0|_{\eta\to\infty}$ be equal to $\Theta|_{y_{j'}\to 0}$, and that a part of $\Theta_1|_{\eta\to\infty}$ match the gradient

$$(\partial\Theta/\partial y_{j'})|_{y_{j'}\to 0}.$$

Also noting that $4\Theta_0^3\Theta_1|_{\eta\to\infty}$ matches $(\partial\Theta^4/\partial y_{j'})_{y_{j'}\to 0}$, we get

$$F_{g0}|_{\eta\to\infty} \sim f_{g0} - 8\Theta^4|_{y_{j'}\to 0},$$

$$\left(\frac{Bo}{N}\right)^{\frac{1}{2}} F_{g1}|_{\eta\to\infty} \sim \left(\frac{Bo}{N}\right)^{\frac{1}{2}} \left[f_{g1} + \left\{\chi f_{g0} - \frac{8}{\Delta^4} - 8 \frac{\partial\Theta^4}{\partial y_{j'}}\bigg|_{y_j\to 0}\right\} \eta\xi^{\frac{1}{2}}\right]. \tag{A 4}$$

Using asymptotic matching of solution for $F_{j'}$ with the outer limits, (A 4), and noting $y_{j'} = \eta\xi^{\frac{1}{2}}(Bo/N)^{\frac{1}{2}}$, we have

$$F_{j'}|_{y_{j'}\to 0} = f_{g0} - 8\Theta_4|_{y_j\to 0}, \tag{A 5a}$$

$$\left.\frac{\partial F_{j'}}{\partial y_{j'}}\right|_{y_{j'}\to 0} = \chi f_{g0} - \frac{8\chi}{\Delta^4} - 8\left.\frac{\partial \Theta^4}{\partial y_{j'}}\right|_{y_{j'}\to 0}. \tag{A 5b}$$

Eliminating f_{g0} between (A 5a) and (A 5b), we recover the slip boundary condition (see Sparrow & Cess 1966)

$$\frac{\partial}{\partial y_{j'}}\{F_{j'} + 8\Theta^4\}|_{y_{j'}\to 0} = \chi\left\{F_{j'} + 8\left(\Theta^4 - \frac{1}{\Delta^4}\right)\right\}\Bigg|_{y_{j'}\to 0}.$$

Appendix B. A note on the local similarity assumption

The approximate method of local similarity has been used in hypersonic flow theory (Moore 1964), linearized radiating boundary-layer flow (Cess 1966), and buoyancy-induced flows (Nagendra 1971). The approximation simply expresses that, under certain conditions, the boundary layer is relatively insensitive to streamwise pressure gradient and temperature gradients. We carry out below a simple order of magnitude analysis to show that the local similarity approximation can be used advantageously in the present problem.

Expressing the derivatives concerned in terms of (ξ, η) we have

$$\frac{\dfrac{\partial\Theta}{\partial\eta}}{\dfrac{\partial\Theta}{\partial x}} = \frac{\dfrac{\partial\Theta}{\partial\eta}}{\dfrac{1}{BoN}\dfrac{\partial\Theta}{\partial\xi} - \dfrac{\eta}{2x}\dfrac{\partial\Theta}{\partial\eta}}. \tag{B 1}$$

The following are the measures in the boundary layer: (i) $\eta = O(1)$, (ii) $x = O(BoN) \gg 1$, and (iii) $\partial\Theta/\partial\eta$ has a maximum value of order unity. When these are introduced into (B 1), we obtain

$$\frac{\partial\Theta}{\partial\eta}\Big/\frac{\partial\Theta}{\partial x} = O(BoN). \tag{B 2}$$

Unless $Bo \sim N^{-1}$, the above expression will always be very much larger than unity and the temperature variation in the x direction can be handled parametrically. The case $Bo \sim N^{-1}$ has been excluded from the scope of the present study since the continuum approximation itself might become doubtful (see § 2).

REFERENCES

Cess, R. D. 1964 The interaction of thermal radiation with conduction and convection heat transfer. *Advances in Heat Transfer*, vol. 1. Academic Press.

Cess, R. D. 1966 Thermal radiation in boundary layer heat transfer. *Proc. Third Int. Heat Transfer Conf.* vol. V. New York: A.I.Ch.E.

Cheng, P. 1964 Radiating gas flow by a moment method. *A.I.A.A. J.* **2**, 1662.

Curle, N. 1962 *The Laminar Boundary Layer Equations*. Oxford University Press.

Emanuel, G. 1968 Radiative transport in an optically thick planar medium. *Int. J. Heat Mass Transfer* **11**, 1413.

EMANUEL, G. 1970 Application of matched asymptotic expansions to radiative transfer in an optically thick gas. *Proc.* 1970 *Heat Transfer and Fluid Mech. Inst.* Stanford University Press.

HOWARTH, L. 1951 Some aspects of Rayleigh's problem for a compressible fluid. *Quart. J. Mech. Appl. Math.* **4** (2), 157.

KAPLUN, S. 1954 Role of coordinates in boundary layer theory. *Z. angew. Math. Phys.* **2**, 111.

KOCH, W. 1972 Application of Olfe's modified differential approximation to the radiation layer problem on a flat plate. *Int. J. Heat Mass Transfer* **15**, 2663.

KRUSKAL, M. D. 1963 *Mathematical Models in Physical Sciences* (ed. S. Drobot). Prentice Hall.

LICK, W. 1963 Energy transfer by radiation and conduction. *Proc.* 1963 *Heat Transfer and Fluid Mech. Inst.* Stanford University Press.

MOORE, F. K. 1961 On local flat plate similarity in the hypersonic boundary layer. *J. Aero. Sci.* **28**, 753.

NAGENDRA, H. R. 1971 Studies on free convection. Ph.D. thesis, Dept. Mech. Engng, Indian Inst. of Science.

OLFE, D. B. 1967 A modification of the differential approximation for radiative transfer. *A.I.A.A. J.* **5**, 638.

OZISIK, M. N. 1973 *Radiative Transfer and Interactions with Conduction and Convection.* Wiley.

PAI, S. I. & TSAO, C. K. 1966 A uniform flow of a radiating gas over a flat plate. *Proc. Third Int. Heat Transfer Conf.* vol. v. New York: A.I.Ch.E.

RALSTON, A. 1965 *A First Course in Numerical Analysis.* McGraw-Hill.

RALSTON, A. & WILF, H. S. 1960 *Mathematical Methods for Digital Computers.* Wiley.

RAIZER, IU. P. 1957 On the structure of the front of strong shock waves in gases. *Sov. Phys. J. Exp. Theor. Phys.* **5**, 1242.

ROBERTS, S. M. & SHIPMAN, J. S. 1972 *Two Point Boundary Value Problems: Shooting Methods.* Elsevier.

SCHLICHTING, H. 1960 *Boundary Layer Theory.* McGraw-Hill.

SIBULKIN, M. & DENNAR, E. A. 1972 Radiating boundary layers at planetary entry velocities. *Int. J. Heat Mass Transfer* **15**, 619.

SMITH, C. 1957 *A Treatise on Algebra.* Macmillan.

SOLAN, A. & COHEN, I. M. 1967*a* Rayleigh problem in a radiating compressible gas. I. Plate Mach number finite. *Phys. Fluids* **10**, 108.

SOLAN, A. & COHEN, I. M. 1967*b* Rayleigh problem in a radiating compressible gas. II. Plate Mach number large. *Phys. Fluids* **10**, 257.

SPARROW, E. M. & CESS, R. D. 1966 *Radiation Heat Transfer.* Brooks/Cole Publishing Co.

TAITEL, Y. 1969 Exact solution for the 'radiation layer' over a flat plate. *J. Heat Transfer, Trans. A.S.M.E.* C **91**, 188.

USISKIN, C. M. & SPARROW, E. M. 1960 Thermal radiation between parallel plates separated by an absorbing emitting non-isothermal gas. *Int. J. Heat Mass Transfer* **1**, 28.

VAN DYKE, M. 1964 *Perturbation Methods in Fluid Mechanics.* Academic Press.

VENKATESHAN, S. P. 1977 Radiative interaction in boundary layers. Ph.D. thesis, Dept. Mech. Engng, Indian Inst. of Science.

VENKATESHAN, S. P. & KRISHNA PRASAD, K. 1973 Asymptotic forms of radiating boundary layers. Paper no. A-16, *Second Natl. Heat and Mass Transfer Conf.* Ind. Inst. of Tech., Kanpur.

VENKATESHAN, S. P. & KRISHNA PRASAD, K. 1975 Optically thin radiation model in boundary layer flow. HMT-33-75, *Third Natl. Heat and Mass Transfer Conf.* Ind. Inst. of Tech., Bombay.

VENKATESHAN, S. P. & KRISHNA PRASAD, K. 1978 Radiating laminar boundary layer flow over a flat plate at a large free stream Mach number. Paper presented at *Sixth Int. Heat Transfer Conf.* 7–11 Aug. Toronto.

VINCENTI, W. G. & KRUGER, C. H. 1965 *Introduction to Physical Gas Dynamics.* Wiley.

VISKANTA, R. 1966 Radiation transfer and interaction of convection with radiation. *Advances in Heat Transfer*, vol. 3. Academic Press.